ACS Chemical Neuroscience

Article

Enantio-specific Allosteric Modulation of Cannabinoid 1 Receptor

Robert B. Laprairie, Pushkar M Kulkarni, Jeffrey R. Deschamps, Melanie E.M. Kelly, David R. Janero, Maria G. Cascio, Lesley A. Stevenson, Roger G. Pertwee, Terry Kenakin, Eileen M. Denovan-Wright, and Ganesh A Thakur

ACS Chem. Neurosci., **Just Accepted Manuscript** • DOI: 10.1021/acschemneuro.6b00310 • Publication Date (Web): 19 Jan 2017

ACS Publications

ACS Chemical Neuroscience is published by the American Chemical Society. 1155 Sixteenth Street N.W., Washington, DC 20036

Enantio-specific Allosteric Modulation of Cannabinoid 1 Receptor

Robert B. Laprairie[†], Pushkar M. Kulkarni[‡], Jeffrey R. Deschamps[¥], Melanie E.M. Kelly[†,§], David R. Janero[‖], Maria G. Cascio[⊥], Lesley A. Stevenson[⊥], Roger G. Pertwee[⊥], Terrence P. Kenakin[√], Eileen M. Denovan-Wright[†], and Ganesh A. Thakur[‡*]

[†]Departments of Pharmacology and [§]Ophthalmology and Visual Sciences, Dalhousie University, Halifax NS CAN B3H 4R2

[‡]Department of Pharmaceutical Sciences, School of Pharmacy, Bouvé College of Health Sciences, Northeastern University, Boston, MA 02115, USA

[¥]Naval Research Laboratory, Code 6930, 4555 Overlook Avenue, Washington, DC 20375, USA

[‖]Center for Drug Discovery; Department of Pharmaceutical Sciences, School of Pharmacy, Bouvé College of Health Sciences; Department of Chemistry and Chemical Biology, College of Science; and Health Sciences Entrepreneurs; Northeastern University, Boston, MA 02115, USA

[⊥]School of Medicine, Medical Sciences and Nutrition, Institute of Medical Sciences, University of Aberdeen, Aberdeen Scotland UK AB25 2ZD

[√]Department of Pharmacology, University of North Carolina School of Medicine, Chapel Hill, NC 27599, USA

To whom correspondence should be addressed: Ganesh A Thakur, Department of Pharmaceutical Sciences, Northeastern University, 145 The Fenway. Boston MA USA 02115, Tel.: (617) 373-8163; Fax: (617) 373-8886; E-mail: g.thakur@neu.edu

KEYWORDS: *Allosteric regulation, cannabinoid, cellular signaling, central nervous system, G protein-coupled receptor, ligand bias, molecular pharmacology, probe dependence, receptor activation, therapeutics discovery, 7-transmembrane receptor*

ABSTRACT:

The cannabinoid 1 receptor (CB1R) is one of the most widely expressed metabotropic G protein-coupled receptors in brain, and its participation in various (patho)physiological processes has made CB1R activation a viable therapeutic modality. Adverse psychotropic effects limit the clinical utility of CB1R orthosteric agonists and have promoted the search for CB1R positive allosteric modulators (PAMs) with the promise of improved drug-like pharmacology and enhanced safety over typical CB1R agonists. In this study, we describe the synthesis and *in vitro* and *ex vivo* pharmacology of the novel allosteric CB1R modulator GAT211 (racemic) and its resolved enantiomers, GAT228 (*R*) and GAT229 (*S*). GAT211 engages CB1R allosteric site(s), enhances the binding of the orthosteric full agonist [^{3}H]CP55,490 and reduces the binding of the orthosteric antagonist/inverse agonist [^{3}H]SR141716A. GAT211 displayed both PAM and agonist activity in HEK293A and Neuro2a cells expressing human recombinant CB1R (hCB1R) and, in mouse-brain membranes rich in native CB1R. GAT211 also exhibited a strong PAM effect in isolated vas deferens endogenously expressing CB1R. Each resolved and crystallized GAT211 enantiomer showed a markedly distinctive pharmacology as a CB1R allosteric modulator. In all biological systems examined, GAT211's allosteric agonist activity resided with the *R*-(+)-enantiomer (GAT228), whereas its PAM activity resided with the *S*-(-)-enantiomer (GAT229), which lacked intrinsic activity. These results constitute the first demonstration of enantiomer-selective CB1R positive allosteric modulation and set a precedent whereby enantiomeric resolution can decisively define the molecular pharmacology of a CB1R allosteric ligand.

INTRODUCTION

Expressed to varying extents in peripheral tissues, the cannabinoid 1 receptor (CB1R) is the most abundant G protein-coupled receptor (GPCR) in the central nervous system.[1, 2] Naturally-occurring CB1R agonists including the endocannabinoids anandamide (AEA) and 2-arachidonoylglycerol (2-AG) and the plant-derived phytocannabinoid and principal psychoactive cannabis constituent, Δ^9-tetrahydrocannabinol (Δ^9-THC), activate the receptor by engaging its orthosteric site.[1-3] CB1R-dependent signaling directly regulates neurotransmission, synapse formation, nociception, metabolism, and reproduction such that aberrant CB1R-mediated information transmission has been implicated in diverse pathologies associated with these and other physiological processes. Such considerations have spurred the design and biological profiling of chemically-diverse CB1R orthosteric ligands as potential pharmacotherapeutics for treating prevalent unsolved medical problems including neurological/neurodegenerative diseases, chronic pain, substance-use disorders, obesity and diabetes.[3-12] Although a few CB1R orthosteric agonists have gained regulatory approval for select indications[13], their association with untoward psychotropic side effects has severely limited their translational potential and clinical utility, spurring the quest for small-molecule ligands with alternative modes of CB1R pharmacological modulation that would be more attractive for therapeutic application.[14-17]

Allosteric modulators bind to GPCR site(s) that are topographically and structurally distinct from-- yet interact cooperatively with-- those that engage orthosteric ligands.[18] Binding of an allosteric modulator is believed to induce a conformational change in the receptor that affects the receptor's affinity for, and/or the efficacy of, an orthosteric ligand to generate receptor conformational states with unique structural and functional phenotypes.[18-20] Positive allosteric modulators (PAMs) enhance orthosteric ligand binding and/or receptor activity, whereas negative

allosteric modulators (NAMs) reduce orthosteric ligand binding and/or receptor activity. Allosteric agonist- positive allosteric modulators (ago-PAMs) exhibit agonism through allosteric sites to varying degrees, in the absence of an orthosteric ligand in addition to potentiating GPCR activation in the presence of an orthosteric ligand.[21]

As exemplified in Figure 1, structurally distinct, synthetic, plant-derived, and endogenous CB1R allosteric ligands have been identified. The paradigmatic, first-generation CB1R allosteric modulators, Org27569 and PSNCBAM-1, paradoxically enhance the affinity, but reduce the efficacy, of orthosteric cannabinergic ligands such as CP55,940, thus acting as PAMs of binding but NAMs in functional assays.[22-28] Org27569 and PSNCBAM-1 also display some inverse-agonist activity *in vitro*, suggesting that they may not act as "pure" NAMs under certain conditions.[24, 25, 29-31] Fenofibrate, the PPARα agonist, has been shown to act as a CB1R NAM[32] whereas RTI-371, the dopamine transport inhibitor[33], and ZCZ011[34] have been reported to act as CB1R PAMs. Cannabidiol, a non-psychoactive phytocannabinoid with potential therapeutic utility for treating numerous disorders, was recently shown by us to act as a non-competitive CB1R NAM.[35] Putative endogenous CB1R allosteric modulators include the non-classical anti-inflammatory eicosanoid, lipoxin A4, a CB1R PAM of orthosteric ligand binding and adenylyl cyclase activity and an *in vivo* anti-inflammatory agent[2, 27, 36]; the steroid pregnenolone, a NAM of CB1R-mediated ERK1/2 phosphorylation with no effect on orthosteric agonist binding affinity or cAMP-mediated signaling[2, 27, 37]; and a family of hemopressin-related peptide endocannabinoids ("Pepcans") that act as CB1R NAMs.[2, 38] The existence of endogenous CB1R allosteric ligands suggests the importance of allostery to physiological CB1R function and regulation.[39] From a pharmacotherapeutic perspective, CB1R PAMs hold promise of greater clinical utility than typical CB1R orthosteric agonists because of their lack of intrinsic efficacy in the absence of an orthosteric

ligand and their ability to modify the magnitude of the effect with the nature of the orthosteric ligand ("probe-dependence"). Furthermore their inherent efficacy ceiling renders PAMs less likely to elicit the CB1R supraphysiological activation, desensitization, and downregulation identified as causal factors underlying the psychotropic side effects of typical CB1R orthosteric agonists.[14, 21, 34, 40] Ago-PAMs may be particularly attractive for treating disease states whose etiology involves severe loss of endogenous neurotransmitters.[18, 41, 42] Given the therapeutic potential of agents that modulate CB1R activity and the distinctive pharmacological characteristics of GPCR/CB1R allosteric activators, novel, efficacious, potent, and selective small-molecule CB1R PAMs are increasingly being sought.[15, 16, 34]

To address this need, we report the synthesis of GAT211 (**1**), a racemic compound derived from 2-phenylindole, by our recently developed microwave-accelerated methodology (Scheme 1),[43] and its initial pharmacological profiling. GAT211 has one chiral center. Its enantiomers, GAT228 (*R*-(+); **1a**) and GAT229 (*S*-(+); **1b**), were separated by chiral HPLC (Scheme 1) and crystallized, and their absolute stereochemistry was determined using single-crystal X-ray diffraction (Figs 2A & 2B). The three compounds were characterized as allosteric modulators of CB1R orthosteric ligand binding and signaling in cell-based systems overexpressing human CB1R (hCB1R) and in tissues endogenously expressing CB1R. GAT211 displayed properties consistent with both CB1R positive allosteric modulation and CB1R partial agonist activity through an allosteric site as an ago-PAM. The pharmacological profiling of the resolved enantiomers revealed that the allosteric agonist activity was exclusively attributable to GAT228 (*R*-(+) enantiomer), while GAT211's potent PAM activity was attributable to GAT229 (*S*-(-) enantiomer). GAT211, GAT228, and GAT229 thus comprise a unique family of CB1R allosteric modulators with enantiomer-specific activity.

CHEMISTRY:

In general, the Michael addition of 2-phenylindole to nitrostyrene gives the expected addition product, albeit in low yields (Scheme 1). Although this Michael addition reaction proceeds smoothly with indoles lacking a phenyl substitution at C-2 position, the presence of phenyl ring at this position poses significant steric and electronic demand and markedly decreases the rate of addition at the indole ring C-3 position. In line with our interest in developing microwave accelerated methodologies for rapidly constructing libraries of biologically active compounds[41, 44, 45], we recently reported a mild and high yielding microwave-accelerated synthesis of **1** in presence of ammonium trifluooacetate.[43] Recognizing the demand for compound supply required for enantiomer separation and *in vitro* and *in vivo* therapeutic profiling, we utilized this methodology to synthesize **1** on a multi-gram scale and obtained the desired product in 88% yield with 10 minutes of microwave irradiation (Scheme 1). Baseline enantiomeric resolution of racemate **1** was achieved by chiral HPLC under supercritical fluid chromatography (SFC) conditions with CHIRALPAK®IC column (Supporting Information Tables 1-4; Figures 1-3). Both the (+)-enantiomer **1a** (GAT228) and the (-)-enantiomer **1b** (GAT229) were obtained in >99% ee. The circular dichroism (CD) spectra of GAT228 and GAT229 were recorded in chloroform and found to be mirror images of each other, confirming their enantiomeric relationship (see Supporting Information, Figure 4).

Crystalline 1a (GAT228) and 1b (GAT229) and Stereochemical Assignments. To obtain absolute configuration of the chiral center in **1a** and **1b**, we explored different crystallization conditions and found that crystals suitable for X-ray investigation were obtained when these enantiomers were crystallized from MeOH:H_2O. Absolute configuration was assigned using

likelihood methods in PLATON. Compounds **1a** and **1b** were found to have (*R*)- and (*S*)- absolute stereochemistry, respectively (Scheme 1; Figures 2A-2B).

RESULTS

GAT211 Acts as a CB1 PAM on Mouse Vas Deferens. The release of contractile transmitters from neurons innervating mouse vas deferens smooth muscle is inhibited by neuronal CB1Rs activation, making inhibition of electrically-evoked vas deferens contractions a well-accepted, *ex vivo* functional assay for CB1R activity.[46] GAT211 (1 μM) potentiated the inhibition of electrically-evoked vas deferens contractions induced by AEA (10 and 100 nM) (Figure 3). By itself, GAT211 had no statistically significant effect on electrically-evoked contractions of the vas deferens at concentrations of 1 nM up to 10 μM (n=6; data not shown). These data suggest that GAT211 enhanced AEA-dependent activation of CB1R in mouse isolated vas deferens, as expected of a CB1R PAM, but itself did not behave as an agonist of CB1Rs naturally expressed in vas deferens.

Effects of GAT Compounds on CB1R Orthosteric Ligand Dissociation and Binding. The effect of GAT211 on CB1R ligand dissociation kinetics was assessed in mouse brain membranes. As compared to vehicle (DMSO) alone, GAT211 (1 μM) increased the $t_{½}$ for [^{3}H]CP55,940 dissociation from mouse brain CB1R (Figure 4): [$t_{½}$ DMSO = 6.1 (4.0-13.1) min; $t_{½}$ GAT211 = 22.4 (15.0-44.2) min; non-overlapping 95% CIs]. The increased binding time (*i.e.* reduced rate of dissociation) is consistent with the allosteric enhancement of orthosteric ligand binding, as would be expected if GAT211 was acting as a PAM.

The effect of GAT211 and its enantiomers GAT228 and GAT229 on CB1R orthosteric ligand binding was assessed in membranes isolated from CHO cells expressing recombinant hCB1R. GAT211 enhanced [^{3}H]CP55,940 binding at 100 nM and 1 μM to CHO-hCB1R membranes (Figure 5A) and from 1 nM – 10 μM to mouse brain membranes (see Supporting Information, Figure 5). The effect of GAT211 on the binding of orthosteric antagonist/inverse agonist [^{3}H]SR141716A to hCB1R was assessed in CHO-hCB1R membranes. GAT211 markedly reduced [^{3}H]SR141716A binding at 1 and 10 μM (Figure 5B). The (+)-enantiomer, GAT228 had no effect on [^{3}H]CP55,940 binding up to 1 μM in CHO-hCB1R cell membranes (Figure 5C), but showed a weak PAM effect at a 10 μM concentration. GAT229 (1 nM – 10 μM, Figure 5D) enhanced [^{3}H]CP55,940 binding to CHO-hCB1R membranes to a far greater extent than GAT228 and to a slightly greater extent than GAT211. The decrease in PAM effect on binding observed in 5A and 5D at supra-pharmacological concentration (10 μM) was due to the limited solubility in these preparations. GAT211-dependent displacement of [^{3}H]CP55,940 was also assessed in CHO-hCB2R membranes. GAT211 had no effect on [^{3}H]CP55,940 binding to hCB2R up to 1μM, and increased [^{3}H]CP55,940 binding by only 29% at a supra-pharmacological concentration of 10 μM (data not shown).

The overall data in Figure 5 are consistent with racemic GAT211 acting as a CB1R PAM of orthosteric ligand binding. Between its enantiomers, GAT229 behaved as a PAM of orthosteric ligand binding and enhanced [^{3}H]CP55,940 binding more than GAT211 or GAT228.

Concentration-Dependent Effects of GAT211, GAT228, and GAT229 on Signaling in HEK293A Cells. GAT211 and its enantiomer GAT229 significantly enhanced the binding of orthosteric agonist to hCB1R demonstrating their activity as CB1R PAMs. Next, the ability of

GAT211 and its enantiomers to modulate hCB1R-dependent arrestin recruitment and $G\alpha_{i/o}$-dependent inhibition of cAMP production was assessed. HEK293A cells expressing hCB1R-GFP^2 and arrestin2-Rluc were treated with 1 nM – 10 μM CP55,940 with or without 1 nM – 10 μM GAT211, GAT228, or GAT229. CB1R-dependent, agonist-induced (*i.e.* CP55,940) arrestin2 recruitment was then quantified by BRET^2 (Figures 6A-C). CB1R is preferentially coupled to $G_{i/o}$ such that CB1R activation inhibits adenylyl cyclase-mediated cell signaling. The ability of GAT211 and its enantiomers to modulate CB1R-dependent, CP55,940-induced inhibition of cAMP production was thus determined. For this purpose, HEK-CRE cells transfected with hCB1R-GFP^2 were treated with 1 nM – 10 μM CP55,940 in the absence or presence of 1 nM – 10 μM GAT211, GAT228, or GAT229, and cellular cAMP content was quantified (Figure 6D-F). The observed concentration-response data were fit to the allosteric binding model[47, 48] combined with the Black-Leff operational model for agonism.[22, 49, 50] Induced signaling bias by GAT211, GAT228 and GAT229 was estimated through the calculation of $\Delta\text{Log}(\alpha\beta)$.[51]

Four independent estimates of α, β, K_B and τ_B were made for each test compound and signaling pathway examined (Table 1). The resulting data indicate that GAT211 and GAT229 displayed robust PAM activity as demonstrated by $\text{Log}(\alpha\beta)$ values > 0. Calculation of $\Delta\text{Log}(\alpha\beta)$ values (Table 2) with statistical analysis showed that GAT229 evidenced a 2-fold bias in CP55,940 signaling toward inhibition of cAMP production over arrestin2 recruitment (BRET^2).

GAT228 did not exhibit allosteric potentiation on inhibition of cAMP production but showed very weak PAM effect on arrestin2 recruitment (BRET^2). GAT211, which is a 1:1 racemic mixture of the two enantiomers produced no bias in signaling. The direct efficacy of the allosteric modulator (τ_B) is reported as a fraction of the efficacy of CP55,940. Therefore, as seen in Fig. 6B and 6E, GAT228 exhibited allosteric agonism at CB1R as it increased basal arrestin2 recruitment and

cAMP inhibition on its own but did not compete with CP55,940. No such effects were observed with GAT229 in both these assays suggesting it's 'pure' PAM activity at the CB1R.

Effects of GAT211, GAT228, and GAT229 on Agonist-induced, CB1R-dependent Arrestin2 Recruitment with a BRET-based Cell Assays. Modulation of hCB1R-dependent arrestin2 recruitment by the GAT compounds was assessed further in HEK293A and Neuro2a cells transfected with hCB1R-GFP[2] and arrestin2-Rluc, the former cells expressing recombinant hCB1R, and the Neuro2a cells expressing native receptor. The cells were treated with 1 nM – 10 μM 2-AG, AEA, or CP55,940 in the presence or absence of 1 μM GAT211, GAT228, or GAT229. Agonist-induced arrestin2 recruitment to hCB1R was then quantified by BRET[2]. The observed concentration-response data were fitted and analyzed using the non-linear regression (4 parameter) model. GAT211 (1 μM) shifted the BRET[2] concentration-response curves (CRC) leftward and upward in the presence of 2-AG, AEA, and CP55,940 in HEK293A (Figures 7A-C) and Neuro2a (Figures 7E-7G) cells. GAT228 (1 μM) did not shift the BRET[2] CRC relative to orthosteric ligands alone (Figure 7). GAT229 (1 μM) shifted the BRET[2] CRCs of 2-AG, AEA, and CP55,940 leftward and upward in HEK293A (Figures 7A-C) and Neuro2a (Figures 7E-G) cells to a greater degree than GAT211. In HEK293A or Neuro2a cells, both GAT211 and GAT228 increased arrestin2 recruitment in a concentration-dependent manner, whereas GAT229 had no effect (Figures 7D, H). Therefore, the racemic GAT211 demonstrated mixed PAM/allosteric agonist activity for arrestin2 recruitment in both HEK293A and Neuro2a cells as induced by both synthetic (CP55,940) and endogenous (2-AG, AEA) cannabinoids. The allosteric agonist activity attributed to GAT228 contrasts with GAT229's profile in these cell-based systems as a "pure" CB1R PAM.

Effect of GAT compounds on CB1R-Mediated ERK1/2 and PLCβ3 Phosphorylation. GAT211-dependent modulation of CB1R-dependent signaling was further profiled in HEK293A cells expressing recombinant hCB1R and transfected with hCB1R-GFP[2] and Neuro2a cells endogenously expressing CB1R. The cells were treated with 1 nM – 10 μM 2-AG, AEA, or CP55,940 in the presence or absence of 1 μM GAT211, GAT228, or GAT229. ERK (Figure 8) and PLCβ3 (Figure 9) phosphorylation were quantified by In-cell™ western analysis. The observed concentration-response data were fit and analyzed using the non-linear regression (4-parameter) model. As observed for arrestin2 recruitment (Figure 7), GAT211 (1 μM) shifted ERK and PLCβ3 CRCs leftward and upward in the presence of 2-AG, AEA, and CP55,940 in HEK293A (Figures. 8A-C, 9A-C) and Neuro2a (Figures 8E-8G, 9E-9G) cells. GAT228 (1 μM) did not shift the CRCs relative to orthosteric ligands alone (Figures 8 and 9). GAT229 (1 μM) shifted the CRCs leftward and upward in the presence of 2-AG, AEA, and CP55,940 in HEK293A (Figures 8A-C, 9A-C) and Neuro2a (Figures. 8E-G, 9E-G) cells to a greater extent than GAT211. GAT211 or GAT228 (1 nM – 10 μM) increased ERK and PLCβ3 phosphorylation in a concentration-dependent manner, whereas GAT229 was without effect (Figures 8D and 8H, 9D and 9H). These data provide additional evidence that GAT211 acts as a mixed CB1R PAM/allosteric agonist; GAT228 acts as an allosteric partial agonist; and GAT229 acts as a CB1R PAM.

Allosteric Potencies and Efficacies of GAT Compounds in BRET[2] based cell assay and on ERK and PLCβ3 Phosphorylation. The allosteric potencies of GAT211, GAT228, and GAT229 were estimated in HEK293A cells transfected with hCB1R and treated with 500 nM CP55,940 and 1 nM – 10 μM GAT211, GAT228, or GAT229 (Fig. 10, Table 3). Similar experiments were also conducted with 500 nM 2-AG or AEA plus 1 nM – 10 μM GAT211, GAT228, or GAT229 (Table

4). GAT229 was a more potent enhancer of arrestin2 recruitment (Fig. 10A), ERK (Fig. 10B) and PLCβ3 phosphorylation (Fig. 10C) than GAT211 or GAT228 (Table 3).

No difference in respective potencies was observed between the arrestin2 recruitment and PLCβ3 phosphorylation assays among GAT211, GAT228, or GAT229 (Table 3). When data from those assays were pooled and orthosteric ligands were compared, GAT229 was also a more potent enhancer of 2-AG, AEA, and CP55,940-mediated hCB1R signaling than either GAT211 or GAT228 (Table 4). No difference in potency among the GAT compounds was observed whether 2-AG, AEA, or CP55,940 was the orthosteric agonist (*i.e.,* no probe-dependent difference in potency was evident) (Table 4).

The efficacies of GAT211, GAT228, and GAT229 were estimated from the data presented in Figures 7 – 9 and calculated as % E_{max} relative to orthosteric ligand alone (Tables 3 and 4). GAT229 was the more efficacious enhancer of arrestin2 recruitment and PLCβ3 phosphorylation than GAT228 in the presence of 500 nM CP55,940 (Table 3). GAT229 was a less efficacious enhancer of ERK phosphorylation than arrestin2 recruitment (Table 3). GAT229 was a more efficacious enhancer of 2-AG, AEA, and CP55,940-mediated hCB1R signaling than either GAT211 or GAT228 (Table 4). E_{max} was greater in the presence of 2-AG and AEA as compared to CP55,940, for GAT211 and GAT228 (*i.e.* GAT211 and GAT228 displayed probe-dependence for 2-AG and AEA over CP55,940) (Table 4). No probe-dependent difference in efficacy was observed for GAT229 (Table 4). These data are consistent with GAT229 acting as a CB1R PAM.

DISCUSSION

In this study, the racemic compound GAT211 and its enantiomers GAT228 (*R*) and GAT229 (*S*) were characterized as CB1R allosteric modulators. GAT211 did not affect ligand binding to CB2R at concentrations below 10 μM, whereas it was very effective at CB1R at nM concentrations. GAT211 enhanced the inhibitory effect of AEA on electrically evoked contractions in mouse isolated vas deferens, but did not by itself inhibit contractions in the vas deferens, suggesting that GAT211 acted as a CB1R PAM in this assay. Radioligand binding analysis demonstrated GAT211 reduced the rate of dissociation of [^{3}H]CP55,940 from hCB1R in mouse brain membranes and enhanced [^{3}H]CP55,940 binding to hCB1R CHO cell membranes, a profile consistent with GAT211's action as a PAM of orthosteric ligand binding. GAT228 had no effect on [^{3}H]CP55,940 binding up to 1 μM, but showed a small enhancement of binding at a supra-pharmacological concentration, whereas GAT229 enhanced [^{3}H]CP55,940 binding to hCB1R CHO membranes, producing a greater enhancement than either GAT211 or GAT228. Neither GAT211, nor its enantiomers competed with [^{3}H]CP55,940 for CB1R binding. Unlike its effect on [^{3}H]CP55,940 binding, GAT211 reduced the binding of the CB1R inverse agonist [^{3}H]SR141716A at 1 to 10 μM. Based on these data, GAT211 may have affected the conformational equilibrium between CB1R in the R* (*i.e.* spontaneously coupled to signaling pathways) and R states (*i.e.* "uncoupled" from intracellular signaling mechanisms).[52, 53] Such a shift would be expected to increase [^{3}H]CP55,940 CB1 binding and signaling, and reduce [^{3}H]SR141716A CB1R binding and inverse signaling.[52, 53]

We tested GAT211 and its enantiomers GAT228 and GAT229 in four different cell-based assays: arrestin2 recruitment (BRET^2), cAMP inhibition, ERK1/2 and PLCβ3 phosphorylation in HEK293A cells. GAT211 displayed properties consistent with both PAM activity and allosteric

agonist activity across assays in the nanomolar range (Tables 3, 4). That is, GAT211 independently increased arrestin2 recruitment, in addition to enhancing each of these effects in the presence of either CP55,940, 2-AG, or AEA. GAT228 consistently displayed partial agonist activity across assays in the nanomolar range (Tables 3, 4), suggesting that GAT228 was a partial allosteric agonist of CB1R. GAT229, on the other hand, displayed no intrinsic efficacy and consistently showed PAM activity in the nanomolar range in all these assays (Tables 3, 4). Together, these data across multiple model systems and assays are consistent with our characterization of GAT211 as a potent CB1R ago-PAM with allosteric agonist activity residing exclusively in the *R*-(+)-enantiomer, GAT228 and *S*-(-)-enantiomer, GAT229 acting as a 'pure' and potent CB1R PAM.

Org27569 and PSNCBAM-1 have remained by far the most studied CB1R allosteric modulators.[22, 23, 25, 26] Org27569 and PSNCBAM-1 paradoxically enhance orthosteric agonist binding to CB1R and reduce orthosteric ligand-dependent signaling: they are PAMs of ligand binding, but NAMs of receptor signaling. GAT211, Org27569, and PSNCBAM-1 are similar in that they enhance CP55,940 binding and reduce SR141716A binding, suggesting both these prototypic allosteric modulators regulate the equilibrium between R and R* CB1R conformations, perhaps through a common allosteric binding site within the receptor.[40, 52, 53]

From a therapeutic perspective, the functional selectivity of allosteric CB1R ligands may lead to the tailoring of new-generation drugs enabling improved treatment strategies and outcomes, were it to be demonstrated that preferred signaling pathways invoke therapeutic effects over adverse events. We characterized GAT211, GAT228, and GAT229 in several distinct cell-signaling pathways – arrestin2, cAMP inhibition and ERK1/2 ($G\alpha_{i/o}$), and PLCβ3 ($G\alpha_q$) – to determine whether these compounds exhibit any functional selectivity.

It can be seen from the data in Table 1 that GAT229 is a PAM for both arrestin2 recruitment ($BRET^2$) and cAMP responses and produces 2-fold bias toward cAMP (*versus* arrestin2 recruitment); this compound has no intrinsic efficacy for either pathway. GAT228 was inactive as a PAM in the cAMP assays with a very minor effect in arrestin2 recruitment. It had comparable intrinsic efficacy for both pathways. GAT211, the ago-PAM induces no bias in signaling between arrestin2 recruitment and inhibition of cAMP and had comparable intrinsic efficacy for both pathways.

Allosteric modulators can be probe-dependent, that is, the efficacy of the allosteric modulator can vary with the orthosteric probe being used.[54] Previous studies have reported that Org27569 and PSNCBAM-1 both display probe-dependence because they are more potent modulators of CP55,940 binding and CB1R activation than WIN 55,212-2.[25] We employed in this study 2-AG, AEA, and CP55,940 as orthosteric probes because 2-AG and AEA are the major endocannabinoids and CP55,940 is a standard, high potency/efficacy synthetic cannabinergic ligand routinely used for studying CB1R activation.[55] GAT211 and GAT228 displayed probe-dependence as more potent and efficacious enhancers of endocannabinoid (2-AG and AEA) signaling than CP55,940 signaling ($BRET^2$ arrestin2 assay, cAMP assay). GAT229 did not display probe-dependence. These data indicate the PAM activity of GAT211, and to a lesser extent GAT228, may be best observed in the presence of endocannabinoids, whereas GAT229 remains highly active as a CB1R PAM with either endo- or exocannabinoids as the orthosteric agonist. One major reason CB1R allosteric modulators are attractive as potential therapeutics is that they would be less likely to promote psychotropic side-effects elicited by orthosteric CB1R ligands.[14, 21, 54] The observation that GAT211 and its enantiomers are highly active allosteric modulators when endocannabinoids are used as orthosteric agonists holds therapeutic promise because these agents

may effectively enhance endogenous CB1R signaling in the absence of any exogenously administered CB1R orthosteric cannabimimetics that may incite such adverse response. Although inhibition of the two principal hydrolases that degrade endocannabinoids elevates the tissue content of these mediators, prolonged pharmacological or genetic monoacylglycerol lipase ablation drives functional downregulation of CB1R signaling and incite adverse central nervous system effects (tolerance, dependence)[56, 57] and fatty acid amide hydrolase inhibitors have met with high-profile failures in the clinic.[58] Thus, allosteric CB1R activation by GAT211 and its enantiomers could represent a more attractive therapeutic strategy for enhancing endogenous cannabinergic activity than targeting endocannabinoid-degrading enzymes with small-molecule inhibitors.

CONCLUSION

Positive allosteric CB1R modulators have the potential to treat several unsolved medical problems including addiction, glaucoma, neurodegenerative diseases, pain, and neurological disorders without the on-target side effects that have limited the therapeutic utility of direct CB1R orthosteric agonists, antagonists and inverse agonists.[21] In this study, the racemic compound GAT211, and its enantiomers GAT228 and GAT229 were characterized for the first time in an array of biochemical and functional, cell-based assays. GAT211 behaved as a PAM of CB1R that enhanced both [^{3}H]CP55,940 binding and agonist-mediated CB1R signaling. GAT211 also displayed allosteric agonist activity in some assays. The PAM and allosteric agonist activity were attributable to specific GAT211 enantiomer. GAT229 (*S*) was a potent CB1R PAM and GAT228 (*R*) was an allosteric partial agonist at CB1R. To our best knowledge, this study represents the first identification of two enantiomers of a CB1R allosteric ligand having unique molecular pharmacology profiles that make GAT211, GAT228, and GAT229 a set of novel allosteric modulators with potential therapeutic utility.

METHODS

Chemical Synthesis of GAT211 and Separation of Enantiomers. In a 20-mL glass tube, 2-phenylindole (3.0 g, 1.0 eq.), nitro styrene (3.0 g, 1.3 eq.) and CF_3COONH_4 (0.6 g, 0.25 eq.) were taken in 12 mL of 25% aq. EtOH. The tube was sealed, introduced into a microwave reactor, and irradiated for 10 min at 100 ºC with magnetic stirring. After cooling to room temperature, the reaction contents were removed and diluted with cold water followed by extraction with dichloromethane (3x). Combined dichloromethane layer was evaporated under reduced pressure, and the residue was purified by flash chromatography using a Biotage™ SP1 instrument with normal phase GRACE™ columns (40-µm particle size) (Biotage USA, Charlotte, NC) with hexane: acetone (95:5→70:30 gradient) as eluent to give pure product (4.68 g, 88% yield) (Scheme 1). Enantiomers of GAT211 were separated by supercritical fluid chromatography using a 5-mm CHIRALPAK®IC/SFC column with 20% isopropyl acetate as co-solvent at a flow rate of 2 mL/min. Absorbance was measured at 298 nm (Supplementary Tables 1 – 4; Supplementary Figs. 1 – 3). Enantiomer separation and enantiomeric purity was confirmed by HPLC and optical rotations and CD spectra were recorded. (Supplementary Fig. 4).

GAT211 (**1**): ^{1}H NMR (500 MHz, $CDCl_3$) δ 8.15 (s, 1H), 7.52 (d, J = 8.0 Hz, 1H), 7.49-7.41 (m, 5H), 7.39 (d, J = 8.0 Hz, 1H), 7.37-7.26 (m, 4H), 7.26-7.18 (m, 2H), 7.11 (ddd, J = 8.5 Hz, 7.5 Hz, 1.0 Hz, 1H), 5.32 (dd as t, J = 8.0 Hz, 1H), 5.19 (dd, J = 12.5 Hz, 7.5 Hz, 1H), 5.13 (dd, J = 12.5 Hz, 8.5 Hz, 1H). ^{13}C NMR (126 MHz, $CDCl_3$) δ: 140.16, 137.24, 136.32, 132.44, 128.24, 128.17, 129.07, 128.91, 127.75, 127.47, 127.29, 122.77, 120.59, 120.23, 111.69, 109.84, 79.35, 41.06. M.P. = 147-148ºC. MS (ESI) (m/z): 343 $[M+H]^+$. HRMS m/z calculated for C22H18N2O2 $[M]^+$ 342.1368, found 342.1364

GAT228 (**1a**): ^{1}H NMR (500 MHz, $CDCl_3$) δ 8.14 (s, 1H), 7.52 (d, *J* = 8.0 Hz, 1H), 7.49-7.40 (m, 5H), 7.38 (d, *J* = 8.5 Hz, 1H), 7.36-7.26 (m, 4H), 7.26-7.17 (m, 2H), 7.11 (t, *J* = 7.5 Hz, 1H), 5.32 (dd as t, 8.0 Hz, 1H), 5.18 (dd, *J* = 12.5 Hz, 7.5 Hz, 1H), 5.13 (dd, *J* = 12.5 Hz, 8.5 Hz, 1H). MS (ESI) (m/z): 343 $[M+H]^+$.

GAT229 (**1b**): ^{1}H NMR (500 MHz, $CDCl_3$) δ 8.15 (s, 1H), 7.52 (d, *J* = 8.0 Hz, 1H), 7.49-7.41 (m, 5H), 7.39 (d, *J* = 8.0 Hz, 1H), 7.36-7.32 (m, 2H), 7.32-7.27 (m, 2H), 7.25-7.19 (m, 2H), 7.11 (ddd, *J* = 8.5 Hz, 7.5 Hz, 1.0 Hz, 1H), 5.32 (dd as t, *J* = 8.0 Hz, 1H), 5.19 (dd, *J* = 12.5 Hz, 7.5 Hz, 1H), 5.13 (dd, *J* = 12.5 Hz, 8.5 Hz, 1H). MS (ESI) (m/z): 343 $[M+H]^+$.

X-ray Crystallographic Analysis of GAT228 and GAT229

Single-crystal X-ray diffraction data on GAT228 and GAT229 were collected using CuKα radiation and a Bruker Platinum-135 CCD area detector. The crystals were prepared for data collection by coating with high viscosity microscope oil. The oil-coated crystal was mounted on a micro-mesh mount (Mitergen, Inc.), transferred to the diffractometer, and a data set collected at 150°K. The structure was solved by direct methods and refined by full-matrix least squares on F^2 values using the programs found in the SHELXTL suite (Bruker, SHELXTL v6.10, 2000, Bruker AXS Inc., Madison, WI). Corrections were applied for Lorentz, polarization, and absorption effects. Parameters refined included atomic coordinates and anisotropic thermal parameters for all non-hydrogen atoms. Hydrogen atoms on carbons were included using a riding model [coordinate shifts of C applied to H atoms] with C-H distance set at 0.96 Å. The absolute configuration was evaluated using likelihood methods in PLATON.

For GAT228 a 0.205 x 0.010 x 0.005 mm^3 crystal was monoclinic in space group P 2_1, with unit cell dimensions a = 7.8877(3), b = 13.5114(6), c = 8.1120(3) Å, and β = 99.225(1)°. Data was 95.6% complete to 68.17° θ (~ 0.83 Å) with an average redundancy of 1.99. The final anisotropic full matrix least-squares refinement on F^2 with 236 variables and one restraint converged at R1 = 3.40%, for the observed data and wR2 = 9.22% for all data. The analysis of 924 Bivjot pairs indicated that the absolute structure had been correctly assigned. The method calculated that the probability that the structure is inverted is smaller than 2×10^{-13}. Based on this analysis the absolute configuration at C8 = R (as reported by PLATON) (Figure 2A). Complete information on data collection and refinement is available in the supplemental material (SI-TABLES 5-10).

For GAT229 a 0.243 x 0.107 x 0.092 mm^3 crystal was monoclinic in space group P 2_1, with unit cell dimensions a = 7.8891(3), b = 13.4883(6), c = 8.1151(3) Å, and β = 99.192(1)°. Data was 95.8% complete to 68.02° θ (~ 0.83 Å) with an average redundancy of 1.99. The final anisotropic full matrix least-squares refinement on F^2 with 236 variables and one restraint converged at R1 = 3.03%, for the observed data and wR2 = 8.00% for all data. The analysis of 916 Bivjot pairs indicated that the absolute structure had been correctly assigned. The method calculated that the probability that the structure is inverted is smaller than 1×10^{-22}. Based on this analysis the absolute configuration at C8 = S (as reported by PLATON) (Figure 2B). Complete information on data collection and refinement is available in the supplemental material (SI-Tables 11-16). Atomic coordinates for GAT228 and GAT229 have been deposited with the Cambridge Crystallographic Data Centre (deposition numbers 1504064 and 1504065). Copies of the data can be obtained, free of charge, on application to CCDC, 12 Union Road, Cambridge, CB2 1EZ, UK [fax: +44(0)-1223-336033 or e-mail: deposit@ccdc.cam.ac.uk.

Commercial Chemicals and Reagents. 2-AG, AEA, (-)-*cis*-3-[2-hydroxy-4-(1,1-dimethylheptyl)phenyl]-*trans*-4-(3-hydroxypropyl)cyclohexanol (CP,55,940), and *N*-(Piperidin-1-yl)-5-(4-chlorophenyl)-1-(2,4-dichlorophenyl)-4-methyl-1*H*-pyrazole-3-carboxamide-hydrochloride (SR141716A) were purchased from Tocris Bioscience (Bristol, UK) *Pertussis* toxin (PTx) was purchased from Sigma-Aldrich (Oakville, ON, CAN). Cannabinoids were dissolved in DMSO (final DMSO concentration 0.1% by volume in all assay media) and added directly to tissue-culture media at the concentrations and times indicated. No effects of vehicle alone were observed as compared to culture media alone in any of the assays conducted. PTx was dissolved in dH_2O (50 ng/mL) and added directly to culture media 24 h prior to compound treatment.

***In Vitro* Pharmacology:**

Animals. Adult male MF1 albino mice were purchased from Harlan UK Ltd. (Blackthorn, UK). These mice were maintained on a 12/12 h light/dark cycle with free access to food and water. All animal care and experimental procedures complied with the UK Animals (Scientific Procedures) Act, 1986, and associated guidelines for the use of experimental animals.

Plasmids. hCB1R-green fluorescent protein^2 (GFP^2) and human arrestin2 (β-arrestin1)-*Renilla* luciferase (Rluc) were cloned as fusion proteins at the C-terminus. hCB1R-GFP^2 was generated using the pGFP^2-N3 plasmid (PerkinElmer, Waltham, MA) as described previously.[59] Arrestin2-Rluc was generated using the pRluc-N1 plasmid (PerkinElmer) as described previously.[60] The GFP^2-Rluc fusion construct and Rluc plasmids have also been described.[59]

Cell Culture. Human embryonic kidney 293A (HEK293A), and murine neuroblast Neuro2a cells were originally from the American Type Culture Collection (Manassas, VA).

CHO cells that stably express hCB1R or human cannabinoid 2 receptor (hCB2R) were constructed as detailed.[25] In brief, CHO cells transfected with cDNA encoding human cannabinoid CB1 or CB2 receptors were maintained at 37°C in Dulbecco's modified Eagle's medium nutrient mixture F-12 HAM, supplemented with 1 mM L-glutamine, 10% fetal bovine serum, 0.6% penicillin–streptomycin and G418 (400 mg/mL). All cells were maintained in a humidified tissue-culture incubator at 37° C under 5% CO_2-95% air in their respective media specified below and were passaged twice a week using a non-enzymatic cell dissociation solution.

HEK293A cells were transfected with 400 ng hCB1R-GFP[2]-expressing plasmid described above using Lipofectamine 2000 according to manufacturer's instructions (Invitrogen, Burlington, Ontario, Canada). The HEK293A and Neuro2a cells were maintained in DMEM supplemented with 10% FBS and 10^4 U/mL Pen/Strep.

HEK293A Cignal Lenti CRE (HEK-CRE) reporter cells were provided by Dr. Christopher J. Sinal (Dalhousie University, Nova Scotia, Canada). HEK-CRE cells stably express the firefly luciferase gene driven by tandem repeat elements of the cAMP transcriptional response element (Qiagen, Toronto, Ontario, Canada). Thus, the luciferase signal is directly proportional to the level of cAMP/protein kinase A (PKA) pathway activity. HEK-CRE cells were maintained at 37°C, 5% CO_2-95% air in DMEM supplemented with 10% FBS, 10^4 U/mL Pen/Strep, and 200 μg/mL puromycin.

CHO and HEK cells do not endogenously express CB1R, whereas Neuro2A cells do.

Membrane Preparations. Mouse forebrain membranes were prepared as detailed.[61] In brief, cells were harvested by scraping, centrifuged, and then frozen as a pellet at -20°C until required. Before use in a radioligand binding assay, cells were defrosted, diluted in Tris buffer (50 mM Tris–HCl and 50 mM Tris–base) and homogenized with a 1 ml hand-held homogenizer.

Vas Deferens Organ-bath Experiments. Vasa deferentia were obtained from adult MF1 mice. The tissues were mounted vertically in 4 mL organ baths. They were then subjected to electrical stimulation of progressively greater intensity, followed by an equilibration procedure in which they were exposed to alternate periods of stimulation (2 min) and rest (10 min) until contractions with consistent amplitudes were obtained.[61] These contractions were monophasic and isometric and were evoked by 0.5 s trains of pulses of 110% maximal voltage (train frequency 0.1 Hz; pulse frequency 5 Hz; pulse duration 0.5 ms). All drug additions were made to the organ baths after the equilibration period and there was no washout between those additions. In some experiments, there was an initial application of GAT211 or its vehicle and this was followed 28 min later by a 2 min period of electrical stimulation at the end of which the lowest of a series of concentrations of the endogenous cannabinoid receptor agonist, AEA, was applied. After a 13 min interval, the tissues were electrically stimulated for 2 min and then subjected to a further addition of AEA. This cycle of drug addition, 13 min rest and 2 min stimulation was repeated without washout, to obtain cumulative CRCs, only one of which was constructed per tissue.[62] A similar procedure was used in experiments in which a series of additions of a set of increasing concentrations of GAT211, were made. Each drug addition was made in a volume of 10 μL.

Dissociation Kinetics

Dissociation kinetic assays were performed with the CB1R agonist [^{3}H]CP55,940 (0.7 nM), 1 mg/mL BSA, and 50 mM Tris buffer containing 0.1 mM EDTA and 0.5 mM $MgCl_2$, pH 7.4, in a total assay volume of 500 µL. We used the "isotopic dilution" method to measure the dissociation rate constant for [^{3}H]CP55,940 from mouse whole brain membranes.[63] [^{3}H]CP55,940 (0.7 nM) was incubated with mouse brain membranes (30 µg) for 60 min at 25 °C. Dissociation was initiated by the addition of 1 µM unlabeled ligand in the presence and absence of the test compound. Dissociation times of 0.5 to 120 min at 25 °C were used. To determine the nonspecific binding, experiments were also performed in the presence of a 1 µM concentration of the unlabeled ligand. Binding was terminated by addition of ice-cold wash buffer (50 mM Tris buffer containing 1 mg/mL BSA) and vacuum filtration using a 24-well sampling manifold (Brandel Cell Harvester; Brandel Inc, Gaithersburg, MD, USA) and Whatman GF/B glass-fiber filters that had been soaked in wash buffer at 4°C for 24 h. Each reaction tube was washed five times with a 4 mL aliquot of buffer. The filters were oven-dried for 60 min and then placed in 5 mL of scintillation fluid (Ultima Gold XR), and radioactivity was quantified by liquid scintillation spectrometry. Specific binding was defined as the difference between the binding that occurred in the presence and absence of 1 µM unlabeled ligand and was 70 to 85% of total binding.

Radioligand Displacement Assays.

The assays were carried out with [^{3}H]CP55,940 or [^{3}H]SR141716A and Tris binding buffer (50 mM Tris–HCl, 50 mM Tris–base, 0.1% BSA, pH 7.4), total assay volume 500 µL, using the filtration procedure described previously.[25, 64] Binding was initiated by the addition of transfected human CB1R or CB2R CHO cell membranes (50 µg protein per well) or of whole-brain

membranes obtained from adult MF1 mice (30 μg protein per well). All assays were performed at 37°C for 60 min before termination by adding ice-cold Tris binding buffer followed by vacuum filtration using a Brandel 24-well sampling manifold and Brandel GF/B filters that had been soaked in wash buffer at 4°C for at least 24 h. Each reaction well was washed six times with a 1.2 mL aliquot of Tris-binding buffer. The filters were oven-dried for 60 min and then placed in 3 mL of scintillation fluid (Ultima Gold XR, PerkinElmer, Seer Green, Buckinghamshire, UK). Radioactivity was quantified by liquid scintillation spectrometry. Specific binding was defined as the difference between the binding that occurred in the presence and absence of 1 μM unlabelled CP55,940 or SR141716A. The concentrations of [^{3}H]CP55,940 and of [^{3}H]SR141716A used in our displacement assays were 0.7 nM and 2 nM, respectively. The compounds under investigation were stored as stock solutions of 10 mM in DMSO, the vehicle concentration in all assay wells being 0.1% DMSO.

Bioluminescence Resonance Energy Transfer^2 (BRET^2). Direct interactions between CB1R and arrestin2 were quantified *via* BRET^2.[65] Cells grown in a 6-well plate were transfected with the CB1R-GFP^2 and arrestin2-Rluc constructs using Lipofectamine 2000, according to the manufacturer's instructions (Invitrogen) and treated as previously described.[35, 60] Briefly, at 48 h post-transfection, cells were washed twice with cold 0.1 M PBS and suspended in BRET buffer [0.1 M PBS supplemented with glucose (1 mg/mL), benzamidine (10 mg/mL), leupeptin (5 mg/mL) and a trypsin inhibitor (5 mg/mL)]. Cells were treated with compounds as indicated. Coelenterazine 400a substrate (50 μM; Biotium, Hayward, CA) was added, and light emissions were measured at 405 nm (Rluc) and 510 nm (GFP^2) using a Luminoskan Ascent plate reader (Thermo Scientific, Waltham, MA), with an integration time of 10s and a photomultiplier tube

voltage of 1200 V. BRET efficiency ($BRET_{Eff}$) represents the efficiency of interaction between donor and acceptor proteins – here the BRET ratio between CB1R-GFP^2 and arrestin2-Rluc – subtracted by the BRET ratio for Rluc alone (*i.e.* $BRET_{min}$) and normalized to the BRET ratio observed for a GFP2-Rluc fusion protein (*i.e.* $BRET_{max}$)[59, 60] and is expressed as a ratio with unitless value (eq. 1)

$$BRET_{Eff} = \frac{(BRET_{sample} - BRET_{min})}{(BRET_{max} - BRET_{min})} \quad \textbf{(1)}$$

In-cell™ Westerns. Cells were fixed for 10 min at room temperature with 4% paraformaldehyde and washed three times with 0.1 M PBS for 5 min each. Cells were incubated with blocking solution (0.1 M PBS, 20% Odyssey blocking buffer, and 0.1% Triton X-100) for 1 h at room temperature. Cells were incubated with primary antibody solutions directed against pERK1/2(Tyr205/185) (1:200), ERK1/2 (1:200), pPLCβ3(S537) (1:500), PLCβ3 (1:1000), (Santa Cruz Biotechnology, Dallas, TX) diluted in blocking solution overnight at 4°C. Cells were washed three times with 0.1 M PBS for 5 min each. Cells were incubated in $IR^{CW700dye}$ or $IR^{CW800dye}$ (1:500; Rockland Immunochemicals, Limerick, PA) and washed three times with 0.1 M PBS for 5 min each. Analyses were conducted using the Odyssey Imaging system and software (version 3.0; Li-Cor, Lincoln, NB).

cAMP Luciferase Reporter Assay. Forty-eight hours after transfection of HEK-CRE cells with hCB1R-GFP^2-expressing plasmid, cells were washed twice with cold 0.1 M PBS and suspended in BRET buffer. Cells were dispensed into 96-well plates (10,000 cells/well) and treated as indicated. Cells were then lysed with passive lysis buffer (Promega, Oakville, ON, CAN) for 20 min at room temperature. Twenty microliters of cell lysate were mixed with luciferase assay reagent (50 μM; Promega), and light emissions were measured at 405 nm using a Luminoskan

Ascent plate reader (Thermo Scientific), with an integration time of 10 s and a photomultiplier tube voltage of 1200 V. Data are presented as % inhibition of cAMP accumulation relative to the E_{max} for the orthosteric agonist alone in the presence of 10 μM forskolin.

Statistical Analyses.

For data related to figures 3, 4, 5, 7, 8, 9 and 10, pharmacological statistics from best-fit CRCs were obtained through non-linear regression models with variable slope (four-parameter) (Prism 6.0; GraphPad Software Inc., San Diego, CA). Most results were calculated as changes from a basal level (zero) of: (i) inhibition of electrically-evoked contractions of the vas deferens; (ii) [^{3}H]CP55,940 or [^{3}H]SR141716A binding; (iii) inhibition of cAMP, (iv) arrestin2 recruitment measured *via* BRET^2, or (v) ERK or PLCβ3 phosphorylation. Prism 5.0 was used to construct sigmoidal log concentration-response curves to analyze dissociation-kinetic data and to calculate values of EC_{50}, E_{min}, E_{max}, means, and the standard error (SEM) and/or 95% confidence interval (CI) of each mean.

For data presented in figure 6: CRCs to CP55,940 for cAMP and BRET were obtained in the absence and presence of a range of concentrations of GAT211, GAT228 and GAT229. The resulting patterns of response were fit to the functional allosteric model which is the allosteric binding model[47, 48] combined with the Black–Leff operational model for agonism (Figure 11).[49] In this model the agonist [A] (CP55,940) binds to the receptor R and functions as a probe of receptor function; the allosteric modulators [B] (GAT test compounds) bind to a separate site on the receptor. The co-binding of these molecules reciprocally changes the affinity of binding of each by a factor α and the efficacy of the agonist through a factor β For example, the equilibrium dissociation constant of the agonist-receptor complex in the absence of modulator binding is K_A,

but in the presence of the modulator it becomes $\alpha^{-1}K_A$. The modulator itself may possess efficacy (denoted τ_B) and may directly produce agonism. The equation for the production of response by an agonist in the presence of an allosteric modulator is given as[22, 48, 50]

$$\text{Response} = \frac{(\tau_A/\mathrm{K_A}(1+\frac{\alpha\beta[\mathrm{B}]}{K_B})+\tau_B[\mathrm{B}]/K_B)E_m}{[\mathrm{A}]/K_A(1+\frac{\alpha[\mathrm{B}]}{\mathrm{K_B}}+\tau_A[\mathrm{A}]\left(K_B+\frac{\alpha\beta[\mathrm{B}]}{K_B}\right)+[\mathrm{B}]/K_B(1+\tau_B)+1)} \quad \textbf{(2)}$$

The variable slope of this model can be derived utilizing the variable slope Black-Leff operational model as[66]:

$$\text{Response} = \frac{\tau_A[A]((\mathrm{K_B}+\alpha\beta[\mathrm{B}])+\tau_B[\mathrm{B}]/K_A)^n E_m}{(\tau_A[\mathrm{A}](K_B+\alpha\beta[\mathrm{B}])+\tau_B[\mathrm{B}]K_A)^n+([\mathrm{A}]K_B+K_AK_B+K_A[\mathrm{B}]+\alpha[\mathrm{A}][\mathrm{B}])^n} \quad \textbf{(3)}$$

Data for the two signaling pathways were fit to obtain values of α, β, K_B and τ_B for each of the test compounds as allosteric modulators of CP55,940 receptor activation. Estimation of possible induced signaling bias by these allosteric modulators also was made through comparison of the allosteric modulation produced by the test compounds for each signaling pathway through calculation of $\Delta\mathrm{Log}(\alpha\beta)$.[51] Statistical assessment of the differences in $\mathrm{Log}(\alpha\beta)$ values were made through calculation of 95% confidence limits of the mean $\mathrm{Log}(\alpha\beta)$ values utilizing a pooled variance.[67]

Statistical analyses included Student's unpaired *t*-test, Student's one-sample *t*-test, one- or two-way analysis of variance (ANOVA), as indicated, using GraphPad. *Post-hoc* analyses were performed using Dunnett's multiple comparisons, Bonferroni's or Tukey's tests, as indicated. Homogeneity of variance was confirmed using Bartlett's test. Data are presented as the mean ± the standard error of the mean, or mean and 95% confidence interval, as indicated, from at least 4 independent experiments. *P* values < 0.05 were considered to be significant.

ASSOCIATED CONTENT:

Supporting Information: Chiral HPLC separation and purity details of enantiomers, specific rotations, circular dichroism (CD) spectra, X-ray crystal data and structure refinement, atomic coordinates and equivalent isotropic displacement parameters, bond lengths and angles, anisotropic displacement parameters, hydrogen coordinates and isotropic displacement parameters and torsion angles for GAT228 and GAT229. This material is available free of charge via the interne

AUTHOR INFORMATION:

Corresponding Author:

Ganesh A Thakur, Department of Pharmaceutical Sciences, Northeastern University, 140 The Fenway. Boston MA USA 02115, E-mail: g.thakur@neu.edu, Phone: 1.617.373.8163, Fax: 1.617.373.8886

Authorship Contributions

Designed research: R.B.L., P.M.K., R.G.P., M.K.M, E.M.D-W, and G.A.T.

Synthesized GAT211and enantiomer characterization: P.M.K.

X-ray crystallography studies: J.R.D.

Conducted experiments: R.B.L., P.M.K., M.G.C. and L.A.C.

Analyzed data and literature and wrote the manuscript: R.B.L., D.R.J, R.G.P, M.E.M.K., T.P.K. E.M.D-W., and G.A.T.

Funding: This work was supported by a partnership grant from CIHR, Nova Scotia Health Research Foundation (NSHRF), and the Huntington Society of Canada (HSC) (ROP-97185) to EDW, a CIHR operating grant (MOP-97768) to MEMK; and grants from NIH/National Eye Institute (EY024717 to GAT, RGP and MEK). RBL is supported by studentships from CIHR, HSC, Killam Trusts, and NSHRF. The X-

ray crystallographic work was supported by the United States National Institutes on Drug Abuse (NIDA) through Interagency Agreement #Y1-DA1101 with the Naval Research Laboratory.

ACKNOWLEDGEMENTS: We are thankful to Arabela Grigorescu from Keck Biophysics Facility at Northwestern University for recording CD spectra, Avinash Chaudhary for his help in chiral separation and ee determination, and Abhijit Kulkarni for helpful comments on the manuscript.

ABBREVIATIONS:

The abbreviations used are: 2-AG, 2-arachidonoylglycerol; AEA, anandamide; ANOVA, analysis of variance; $BRET^2$, bioluminescence resonance energy transfer 2; CB1R, type 1 cannabinoid receptor; CB2R, type 2 cannabinoid receptor; CHO, Chinese hamster ovary; CP55,940, (-)-*cis*-3-[2-Hydroxy-4-(1,1-dimethylheptyl)phenyl]-*trans*-4-(3-hydroxypropyl)cyclohexanol; CRC, concentration-response curve; GFP^2, green fluorescent protein variant 2; HEK293A, human embryonic kidney 293 adherent; PTx, *Pertussis* toxin; Rluc, *Renilla* luciferase; SR141716A, *N*-(Piperidin-1-yl)-5-(4-chlorophenyl)-1-(2,4-dichlorophenyl)-4-methyl-1*H*-pyrazole-3-carboxamide-hydrochloride.

REFERENCES:

[1] Pertwee, R. G., Howlett, A. C., Abood, M. E., Alexander, S. P., Di Marzo, V., Elphick, M. R., Greasley, P. J., Hansen, H. S., Kunos, G., Mackie, K., Mechoulam, R., and Ross, R. A. (2010) International Union of Basic and Clinical Pharmacology. LXXIX. Cannabinoid receptors and their ligands: beyond CB(1) and CB(2), *Pharmacological reviews 62*, 588-631.

[2] Pertwee, R. G. (2015) Endocannabinoids and Their Pharmacological Actions, *Handb Exp Pharmacol 231*, 1-37.

[3] Pertwee, R. G. (2008) Ligands that target cannabinoid receptors in the brain: from THC to anandamide and beyond, *Addict Biol 13*, 147-159.

[4] Pacher, P., Batkai, S., and Kunos, G. (2006) The endocannabinoid system as an emerging target of pharmacotherapy, *Pharmacological reviews 58*, 389-462.

[5] Pacher, P., and Kunos, G. (2013) Modulating the endocannabinoid system in human health and disease--successes and failures, *The FEBS journal 280*, 1918-1943.

[6] Di Marzo, V. (2008) Targeting the endocannabinoid system: to enhance or reduce?, *Nat Rev Drug Discov 7*, 438-455.

[7] Vemuri, V. K., Janero, D. R., and Makriyannis, A. (2008) Pharmacotherapeutic targeting of the endocannabinoid signaling system: drugs for obesity and the metabolic syndrome, *Physiol Behav 93*, 671-686.

[8] Thakur, G. A., Tichkule, R., Bajaj, S., and Makriyannis, A. (2009) Latest advances in cannabinoid receptor agonists, *Expert opinion on therapeutic patents 19*, 1647-1673.

[9] Janero, D. R. (2012) Cannabinoid-1 receptor (CB1R) blockers as medicines: beyond obesity and cardiometabolic disorders to substance abuse/drug addiction with CB1R neutral antagonists, *Expert Opin Emerg Drugs 17*, 17-29.

[10] Aizpurua-Olaizola, O., Elezgarai, I., Rico-Barrio, I., Zarandona, I., Etxebarria, N., and Usobiaga, A. (2016) Targeting the endocannabinoid system: future therapeutic strategies, *Drug Discov Today*.

[11] Dixon, D. D., Sethumadhavan, D., Benneche, T., Banaag, A. R., Tius, M. A., Thakur, G. A., Bowman, A., Wood, J. T., and Makriyannis, A. (2010) Heteroadamantyl cannabinoids, *J Med Chem 53*, 5656-5666.

[12] Thakur, G. A., Palmer, S. L., Harrington, P. E., Stergiades, I. A., Tius, M. A., and Makriyannis, A. (2002) Enantiomeric resolution of a novel chiral cannabinoid receptor ligand, *J Biochem Biophys Methods 54*, 415-422.

[13] Pertwee, R. G. (2012) Targeting the endocannabinoid system with cannabinoid receptor agonists: pharmacological strategies and therapeutic possibilities, *Philos Trans R Soc Lond B Biol Sci 367*, 3353-3363.

[14] Ross, R. A. (2007) Allosterism and cannabinoid CB(1) receptors: the shape of things to come, *Trends Pharmacol Sci 28*, 567-572.

[15] Morales, P., Goya, P., Jagerovic, N., and Hernandez-Folgado, L. (2016) Allosteric Modulators of the CB1 Cannabinoid Receptor: A Structural Update Review, *Cannabis and Cannabinoid Research 1*, 22-30.

[16] Busquets Garcia, A., Soria-Gomez, E., Bellocchio, L., and Marsicano, G. (2016) Cannabinoid receptor type-1: breaking the dogmas, *F1000Res 5*.

[17] Abood, M. E. (2016) Allosteric Modulators: A Side Door, *J Med Chem 59*, 42-43.

[18] Lindsley, C. W., Emmitte, K. A., Hopkins, C. R., Bridges, T. M., Gregory, K. J., Niswender, C. M., and Conn, P. J. (2016) Practical Strategies and Concepts in GPCR Allosteric Modulator Discovery: Recent Advances with Metabotropic Glutamate Receptors, *Chem Rev 116*, 6707-6741.

[19] Conn, P. J., Lindsley, C. W., Meiler, J., and Niswender, C. M. (2014) Opportunities and challenges in the discovery of allosteric modulators of GPCRs for treating CNS disorders, *Nat Rev Drug Discov 13*, 692-708.

[20] Gentry, P. R., Sexton, P. M., and Christopoulos, A. (2015) Novel Allosteric Modulators of G Protein-coupled Receptors, *J Biol Chem 290*, 19478-19488.

[21] Wootten, D., Christopoulos, A., and Sexton, P. M. (2013) Emerging paradigms in GPCR allostery: implications for drug discovery, *Nat Rev Drug Discov 12*, 630-644.

[22] Price, M. R., Baillie, G. L., Thomas, A., Stevenson, L. A., Easson, M., Goodwin, R., McLean, A., McIntosh, L., Goodwin, G., Walker, G., Westwood, P., Marrs, J., Thomson, F., Cowley, P., Christopoulos, A., Pertwee, R. G., and Ross, R. A. (2005) Allosteric modulation of the cannabinoid CB1 receptor, *Molecular pharmacology 68*, 1484-1495.

[23] Horswill, J. G., Bali, U., Shaaban, S., Keily, J. F., Jeevaratnam, P., Babbs, A. J., Reynet, C., and Wong Kai In, P. (2007) PSNCBAM-1, a novel allosteric antagonist at cannabinoid CB1 receptors with hypophagic effects in rats, *British journal of pharmacology 152*, 805-814.

[24] Wang, X., Horswill, J. G., Whalley, B. J., and Stephens, G. J. (2011) Effects of the allosteric antagonist 1-(4-chlorophenyl)-3-[3-(6-pyrrolidin-1-ylpyridin-2-yl)phenyl]urea (PSNCBAM-1) on CB1 receptor modulation in the cerebellum, *Mol Pharmacol 79*, 758-767.

[25] Baillie, G. L., Horswill, J. G., Anavi-Goffer, S., Reggio, P. H., Bolognini, D., Abood, M. E., McAllister, S., Strange, P. G., Stephens, G. J., Pertwee, R. G., and Ross, R. A. (2013) CB(1) receptor allosteric modulators display both agonist and signaling pathway specificity, *Molecular pharmacology 83*, 322-338.

[26] Cawston, E. E., Connor, M., Di Marzo, V., Silvestri, R., and Glass, M. (2015) Distinct Temporal Fingerprint for Cyclic Adenosine Monophosphate (cAMP) Signaling of Indole-2-carboxamides as Allosteric Modulators of the Cannabinoid Receptors, *J Med Chem*.

[27] Khajehali, E., Malone, D. T., Glass, M., Sexton, P. M., Christopoulos, A., and Leach, K. (2015) Biased Agonism and Biased Allosteric Modulation at the CB1 Cannabinoid Receptor, *Mol Pharmacol 88*, 368-379.

[28] Gamage, T. F., Ignatowska-Jankowska, B. M., Wiley, J. L., Abdelrahman, M., Trembleau, L., Greig, I. R., Thakur, G. A., Tichkule, R., Poklis, J., Ross, R. A., Pertwee, R. G., and Lichtman, A. H. (2014) In-vivo pharmacological evaluation of the CB1-receptor allosteric modulator Org-27569, *Behav Pharmacol 25*, 182-185.

[29] Shore, D. M., Baillie, G. L., Hurst, D. H., Navas, F., 3rd, Seltzman, H. H., Marcu, J. P., Abood, M. E., Ross, R. A., and Reggio, P. H. (2014) Allosteric modulation of a cannabinoid G protein-coupled receptor: binding site elucidation and relationship to G protein signaling, *The Journal of biological chemistry 289*, 5828-5845.

[30] Laprairie, R. B., Kulkarni, A. R., Kulkarni, P. M., Hurst, D. P., Lynch, D., Reggio, P. H., Janero, D. R., Pertwee, R. G., Stevenson, L. A., Kelly, M. E., Denovan-Wright, E. M., and Thakur, G. A. (2016) Mapping Cannabinoid 1 Receptor Allosteric Site(s): Critical Molecular Determinant and Signaling Profile of GAT100, a Novel, Potent, and Irreversibly Binding Probe, *ACS Chem Neurosci 7*, 776-798.

[31] Kulkarni, P. M., Kulkarni, A. R., Korde, A., Tichkule, R. B., Laprairie, R. B., Denovan-Wright, E. M., Zhou, H., Janero, D. R., Zvonok, N., Makriyannis, A., Cascio, M. G., Pertwee, R. G., and Thakur, G. A. (2016) Novel Electrophilic and Photoaffinity Covalent Probes for Mapping the Cannabinoid 1 Receptor Allosteric Site(s), *J Med Chem 59*, 44-60.

[32] Priestley, R. S., Nickolls, S. A., Alexander, S. P., and Kendall, D. A. (2015) A potential role for cannabinoid receptors in the therapeutic action of fenofibrate, *FASEB journal : official publication of the Federation of American Societies for Experimental Biology 29*, 1446-1455.

[33] Navarro, H. A., Howard, J. L., Pollard, G. T., and Carroll, F. I. (2009) Positive allosteric modulation of the human cannabinoid (CB) receptor by RTI-371, a selective inhibitor of the dopamine transporter, *Br J Pharmacol 156*, 1178-1184.

[34] Ignatowska-Jankowska, B. M., Baillie, G. L., Kinsey, S., Crowe, M., Ghosh, S., Owens, R. A., Damaj, I. M., Poklis, J., Wiley, J. L., Zanda, M., Zanato, C., Greig, I. R., Lichtman, A. H., and Ross, R. A. (2015) A Cannabinoid CB1 Receptor-Positive Allosteric Modulator Reduces Neuropathic Pain in the Mouse with No Psychoactive Effects, *Neuropsychopharmacology 40*, 2948-2959.

[35] Laprairie, R. B., Bagher, A. M., Kelly, M. E., and Denovan-Wright, E. M. (2015) Cannabidiol is a negative allosteric modulator of the cannabinoid CB1 receptor, *Br J Pharmacol 172*, 4790-4805.

[36] Pamplona, F. A., Ferreira, J., Menezes de Lima, O., Jr., Duarte, F. S., Bento, A. F., Forner, S., Villarinho, J. G., Bellocchio, L., Wotjak, C. T., Lerner, R., Monory, K., Lutz, B., Canetti, C., Matias, I., Calixto, J. B., Marsicano, G., Guimaraes, M. Z., and Takahashi, R. N. (2012) Anti-inflammatory lipoxin A4 is an endogenous allosteric enhancer of CB1 cannabinoid receptor, *Proceedings of the National Academy of Sciences of the United States of America 109*, 21134-21139.

[37] Vallee, M., Vitiello, S., Bellocchio, L., Hebert-Chatelain, E., Monlezun, S., Martin-Garcia, E., Kasanetz, F., Baillie, G. L., Panin, F., Cathala, A., Roullot-Lacarriere, V., Fabre, S., Hurst, D. P., Lynch, D. L., Shore, D. M., Deroche-Gamonet, V., Spampinato, U., Revest, J. M., Maldonado, R., Reggio, P. H., Ross, R. A., Marsicano, G., and Piazza, P. V. (2014) Pregnenolone can protect the brain from cannabis intoxication, *Science 343*, 94-98.

[38] Bauer, M., Chicca, A., Tamborrini, M., Eisen, D., Lerner, R., Lutz, B., Poetz, O., Pluschke, G., and Gertsch, J. (2012) Identification and quantification of a new family of peptide endocannabinoids (Pepcans) showing negative allosteric modulation at CB1 receptors, *J Biol Chem 287*, 36944-36967.

[39] van der Westhuizen, E. T., Valant, C., Sexton, P. M., and Christopoulos, A. (2015) Endogenous allosteric modulators of G protein-coupled receptors, *J Pharmacol Exp Ther 353*, 246-260.

[40] Janero, D. R., and Thakur, G. A. (2016) Leveraging allostery to improve G protein-coupled receptor (GPCR)-directed therapeutics: cannabinoid receptor 1 as discovery target, *Expert Opin Drug Discov 11*, 1223-1237.

[41] Thakur, G. A., Kulkarni, A. R., Deschamps, J. R., and Papke, R. L. (2013) Expeditious synthesis, enantiomeric resolution, and enantiomer functional characterization of (4-(4-bromophenyl)-3a,4,5,9b-tetrahydro-3H-cyclopenta[c]quinoline-8-sulfonamide (4BP-TQS): an allosteric agonist-positive allosteric modulator of alpha7 nicotinic acetylcholine receptors, *J Med Chem 56*, 8943-8947.

[42] Bagdas, D., Wilkerson, J. L., Kulkarni, A., Toma, W., AlSharari, S., Gul, Z., Lichtman, A. H., Papke, R. L., Thakur, G. A., and Damaj, M. I. (2016) The alpha7 nicotinic receptor dual allosteric agonist and positive allosteric modulator GAT107 reverses nociception in mouse models of inflammatory and neuropathic pain, *Br J Pharmacol 173*, 2506-2520.

[43] Kulkarni, P. M., Ranade, A., Garai, S., and Thakur, G. A. ((manuscript under review)) Ammonium Trifluoroacetate: A Mild, Efficient and Selective Catalyst for Michael Addition of Substituted Nitrostyrenes to 2-Arylindoles Under Microwave Irradiation. , *J. Het. Chem.* .

[44] Kulkarni, A. R., and Thakur, G. A. (2013) Microwave-assisted Expeditious and Efficient Synthesis of Cyclopentene Ring-fused Tetrahydroquinoline Derivatives Using Three-component Povarov Reaction, *Tetrahedron Lett 54*.

[45] Kulkarni, A. R., Garai, S., and Thakur, G. A. (2016) Scalable, One-Pot, Microwave-Accelerated Tandem Synthesis of Unsymmetrical Urea Derivatives, *J Org Chem*.

[46] Pertwee, R. G., Ross, R. A., Craib, S. J., and Thomas, A. (2002) (-)-Cannabidiol antagonizes cannabinoid receptor agonists and noradrenaline in the mouse vas deferens, *Eur J Pharmacol 456*, 99-106.

[47] Stockton, J. M., Birdsall, N. J., Burgen, A. S., and Hulme, E. C. (1983) Modification of the binding properties of muscarinic receptors by gallamine, *Mol Pharmacol 23*, 551-557.

[48] Ehlert, F. J. (1988) Estimation of the affinities of allosteric ligands using radioligand binding and pharmacological null methods, *Mol Pharmacol 33*, 187-194.

[49] Black, J. W., and Leff, P. (1983) Operational models of pharmacological agonism, *Proc R Soc Lond B Biol Sci 220*, 141-162.

[50] Kenakin, T. (2005) New concepts in drug discovery: collateral efficacy and permissive antagonism, *Nat Rev Drug Discov 4*, 919-927.

[51] Kenakin, T. (2015) Gaddum Memorial Lecture 2014: receptors as an evolving concept: from switches to biased microprocessors, *Br J Pharmacol 172*, 4238-4253.

[52] Barnett-Norris, J., Hurst, D. P., Lynch, D. L., Guarnieri, F., Makriyannis, A., and Reggio, P. H. (2002) Conformational memories and the endocannabinoid binding site at the cannabinoid CB1 receptor, *J Med Chem 45*, 3649-3659.

[53] Pertwee, R. G. (2005) Inverse agonism and neutral antagonism at cannabinoid CB1 receptors, *Life Sci 76*, 1307-1324.

[54] Christopoulos, A., and Kenakin, T. (2002) G protein-coupled receptor allosterism and complexing, *Pharmacological reviews 54*, 323-374.

[55] Sugiura, T., Kodaka, T., Nakane, S., Miyashita, T., Kondo, S., Suhara, Y., Takayama, H., Waku, K., Seki, C., Baba, N., and Ishima, Y. (1999) Evidence that the cannabinoid CB1 receptor is a 2-arachidonoylglycerol receptor. Structure-activity relationship of 2-arachidonoylglycerol, ether-linked analogues, and related compounds, *J Biol Chem 274*, 2794-2801.

[56] Schlosburg, J. E., Blankman, J. L., Long, J. Z., Nomura, D. K., Pan, B., Kinsey, S. G., Nguyen, P. T., Ramesh, D., Booker, L., Burston, J. J., Thomas, E. A., Selley, D. E., Sim-Selley, L. J., Liu, Q. S., Lichtman, A. H., and Cravatt, B. F. (2010) Chronic monoacylglycerol lipase blockade causes functional antagonism of the endocannabinoid system, *Nat Neurosci 13*, 1113-1119.

[57] Schlosburg, J. E., Kinsey, S. G., Ignatowska-Jankowska, B., Ramesh, D., Abdullah, R. A., Tao, Q., Booker, L., Long, J. Z., Selley, D. E., Cravatt, B. F., and Lichtman, A. H. (2014) Prolonged monoacylglycerol lipase blockade causes equivalent cannabinoid receptor type

1 receptor-mediated adaptations in fatty acid amide hydrolase wild-type and knockout mice, *J Pharmacol Exp Ther 350*, 196-204.

[58] Fowler, C. J. (2015) The Potential of Inhibitors of Endocannabinoid Metabolism for Drug Development: A Critical Review, *Handb Exp Pharmacol 231*, 95-128.

[59] Bagher, A. M., Laprairie, R. B., Kelly, M. E., and Denovan-Wright, E. M. (2013) Co-expression of the human cannabinoid receptor coding region splice variants (hCB(1)) affects the function of hCB(1) receptor complexes, *Eur J Pharmacol 721*, 341-354.

[60] Laprairie, R. B., Bagher, A. M., Kelly, M. E., Dupre, D. J., and Denovan-Wright, E. M. (2014) Type 1 cannabinoid receptor ligands display functional selectivity in a cell culture model of striatal medium spiny projection neurons, *J Biol Chem 289*, 24845-24862.

[61] Thomas, A., Ross, R. A., Saha, B., Mahadevan, A., Razdan, R. K., and Pertwee, R. G. (2004) 6"-Azidohex-2"-yne-cannabidiol: a potential neutral, competitive cannabinoid CB1 receptor antagonist, *Eur J Pharmacol 487*, 213-221.

[62] Pertwee, R. G., Fernando, S. R., Griffin, G., Ryan, W., Razdan, R. K., Compton, D. R., and Martin, B. R. (1996) Agonist-antagonist characterization of 6'-cyanohex-2'-yne-delta 8-tetrahydrocannabinol in two isolated tissue preparations, *Eur J Pharmacol 315*, 195-201.

[63] Leach, K., Sexton, P. M., and Christopoulos, A. (2011) Quantification of allosteric interactions at G protein-coupled receptors using radioligand binding assays, *Curr Protoc Pharmacol Chapter 1*, Unit 1 22.

[64] Ross, R. A., Gibson, T. M., Stevenson, L. A., Saha, B., Crocker, P., Razdan, R. K., and Pertwee, R. G. (1999) Structural determinants of the partial agonist-inverse agonist properties of 6'-azidohex-2'-yne-delta8-tetrahydrocannabinol at cannabinoid receptors, *Br J Pharmacol 128*, 735-743.

[65] James, J. R., Oliveira, M. I., Carmo, A. M., Iaboni, A., and Davis, S. J. (2006) A rigorous experimental framework for detecting protein oligomerization using bioluminescence resonance energy transfer, *Nat Methods 3*, 1001-1006.

[66] Black, J. W., Leff, P., Shankley, N. P., and Wood, J. (1985) An operational model of pharmacological agonism: the effect of E/[A] curve shape on agonist dissociation constant estimation, *Br J Pharmacol 84*, 561-571.

[67] Kenakin, T., Watson, C., Muniz-Medina, V., Christopoulos, A., and Novick, S. (2012) A simple method for quantifying functional selectivity and agonist bias, *ACS Chem Neurosci 3*, 193-203.

FIGURE 1

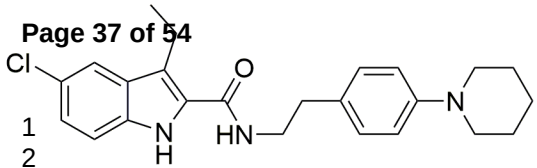

Org27569

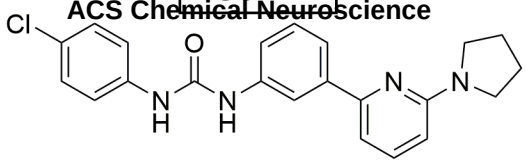

PSNCBAM-1

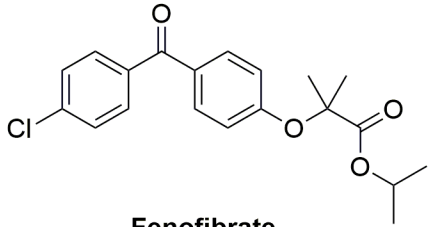

Fenofibrate

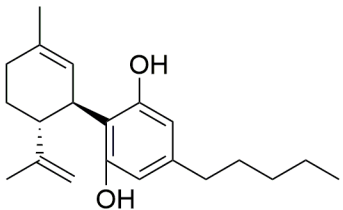

Cannabidiol

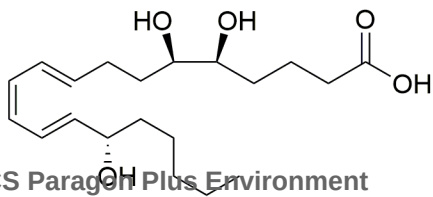

Lipoxin A4

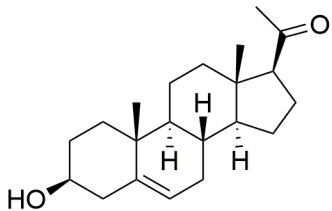

Pregnenolone

FIGURE 2A

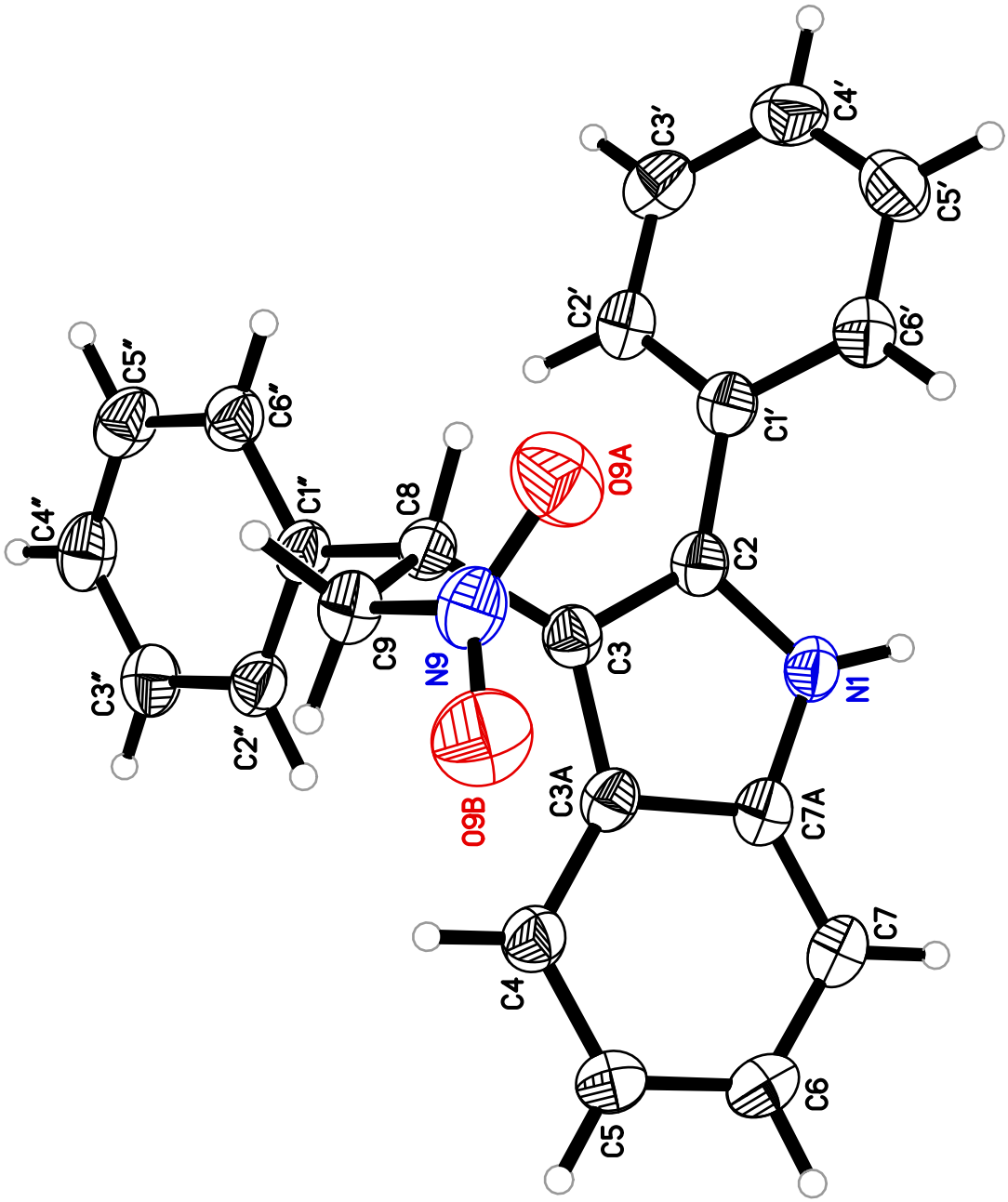
C4′
C3′
C5′
C2′
C6′
C1′
C5″
C6″
C1″
C8
O9A
C2
C4″
C9
N9
C3
N1
C3″
C2″
O9B
C3A
C7A
C7
C4
C6
C5

FIGURE 2B

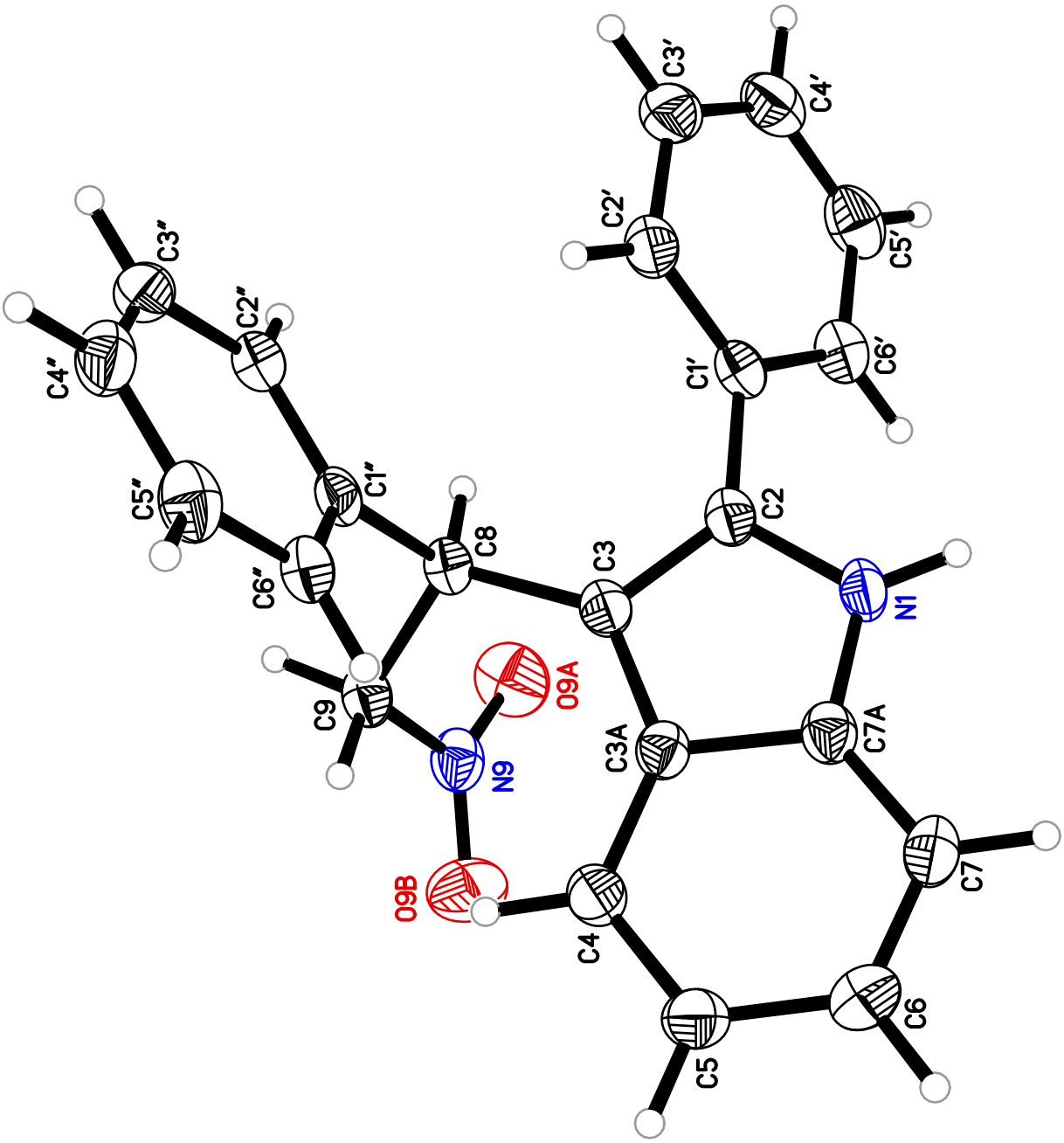
C3′
C4′
C2′
C5′
C1′
C6′
C2
C3
N1
C7A
C3A
C7
C4
C5
C6
C8
C1″
C2″
C3″
C4″
C5″
C6″
C9
N9
O9A
O9B

FIGURE 3

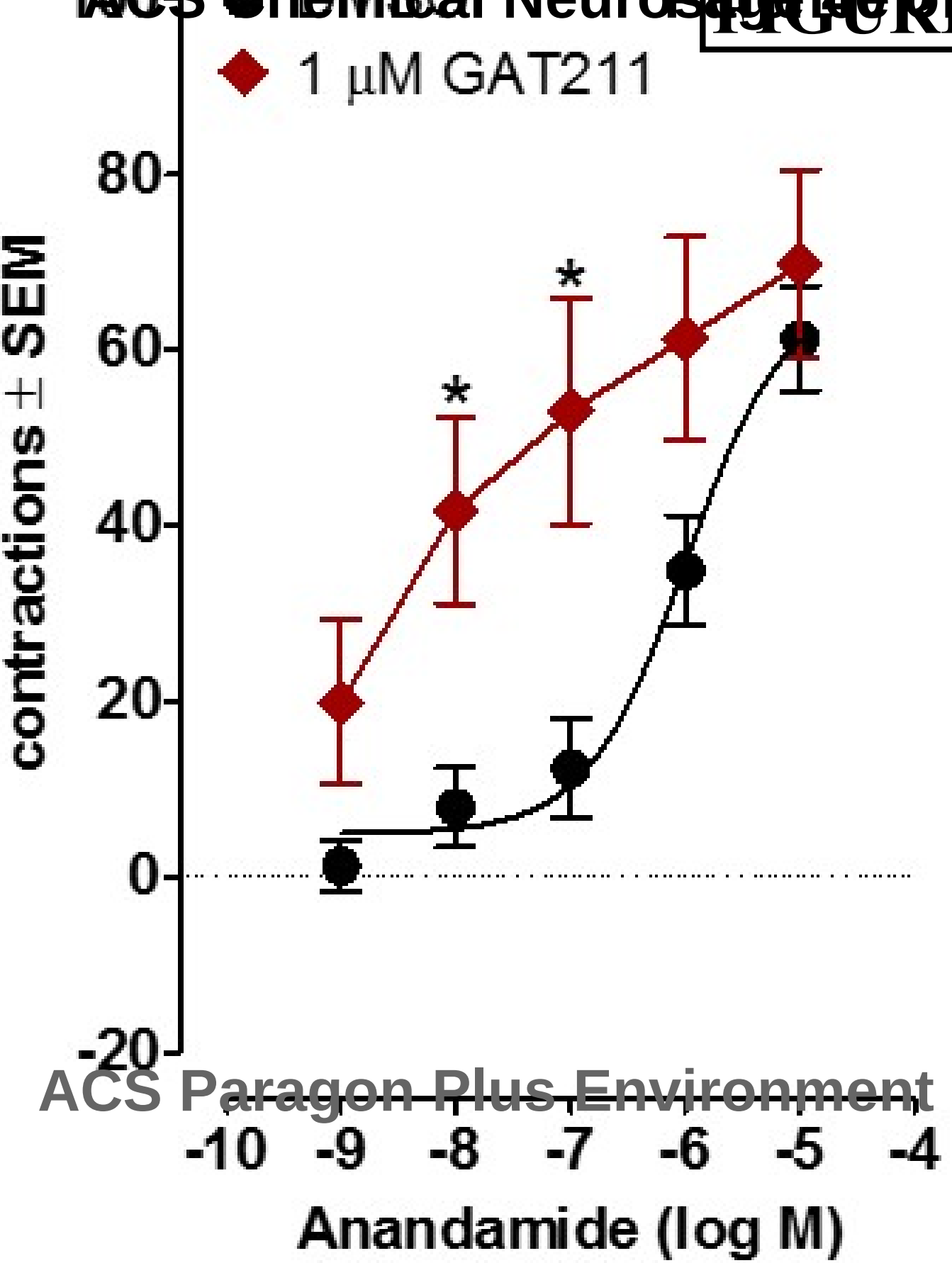

FIGURE 4

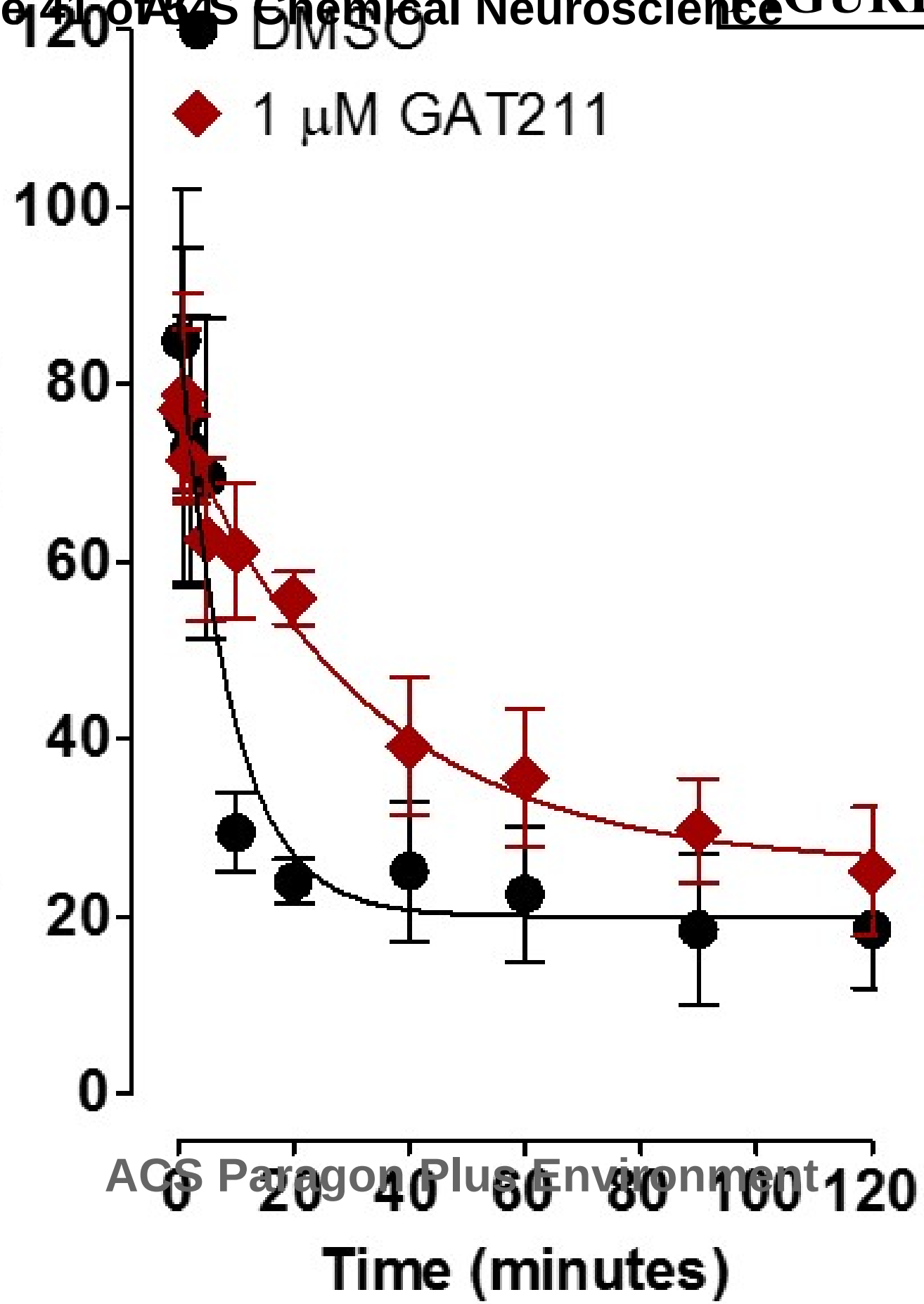

FIGURE 5

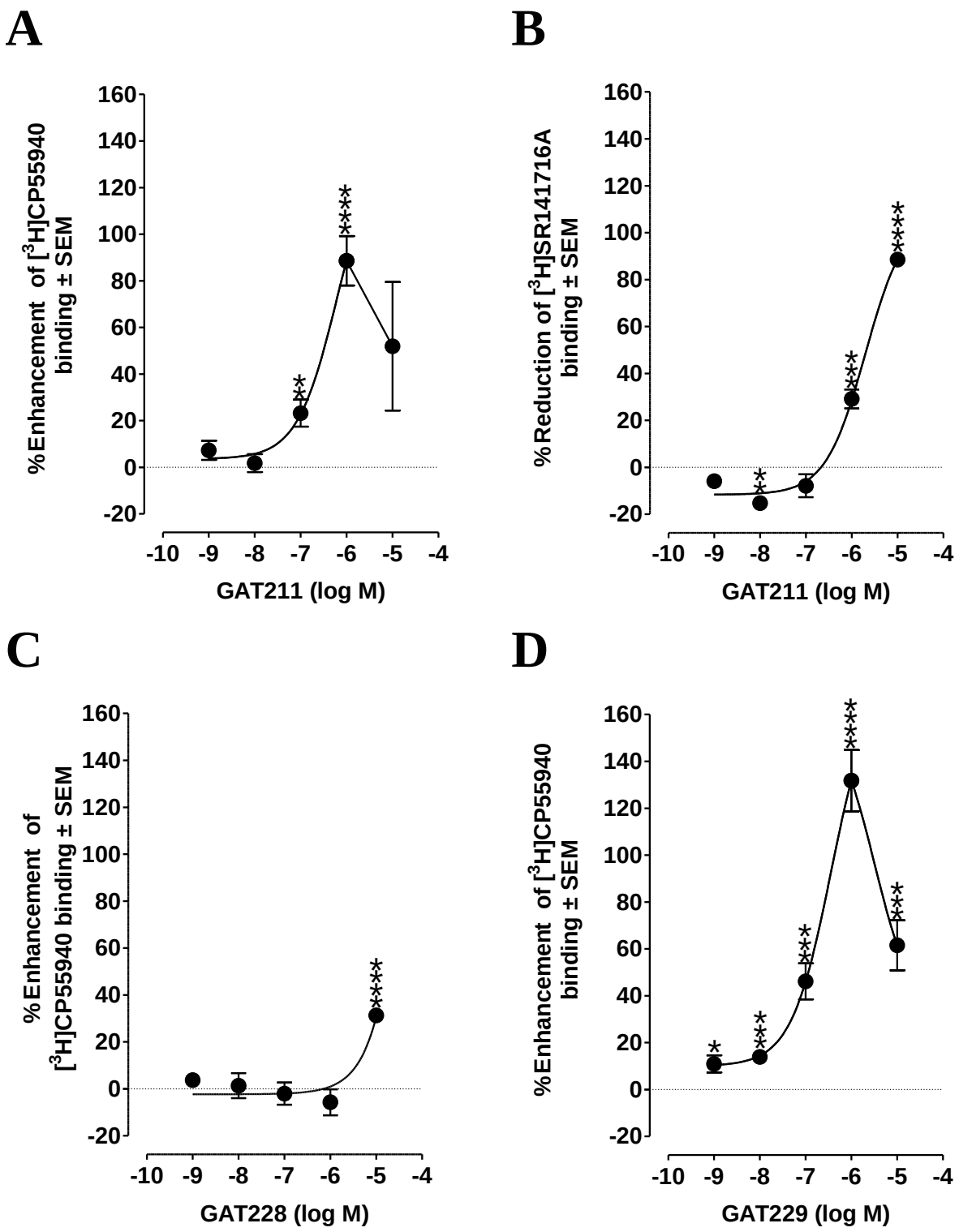
A
%Enhancement of [3H]CP55940 binding ± SEM
GAT211 (log M)
B
%Reduction of [3H]SR141716A binding ± SEM
GAT211 (log M)
C
%Enhancement of [3H]CP55940 binding ± SEM
GAT228 (log M)
D
%Enhancement of [3H]CP55940 binding ± SEM
GAT229 (log M)

Figure 6

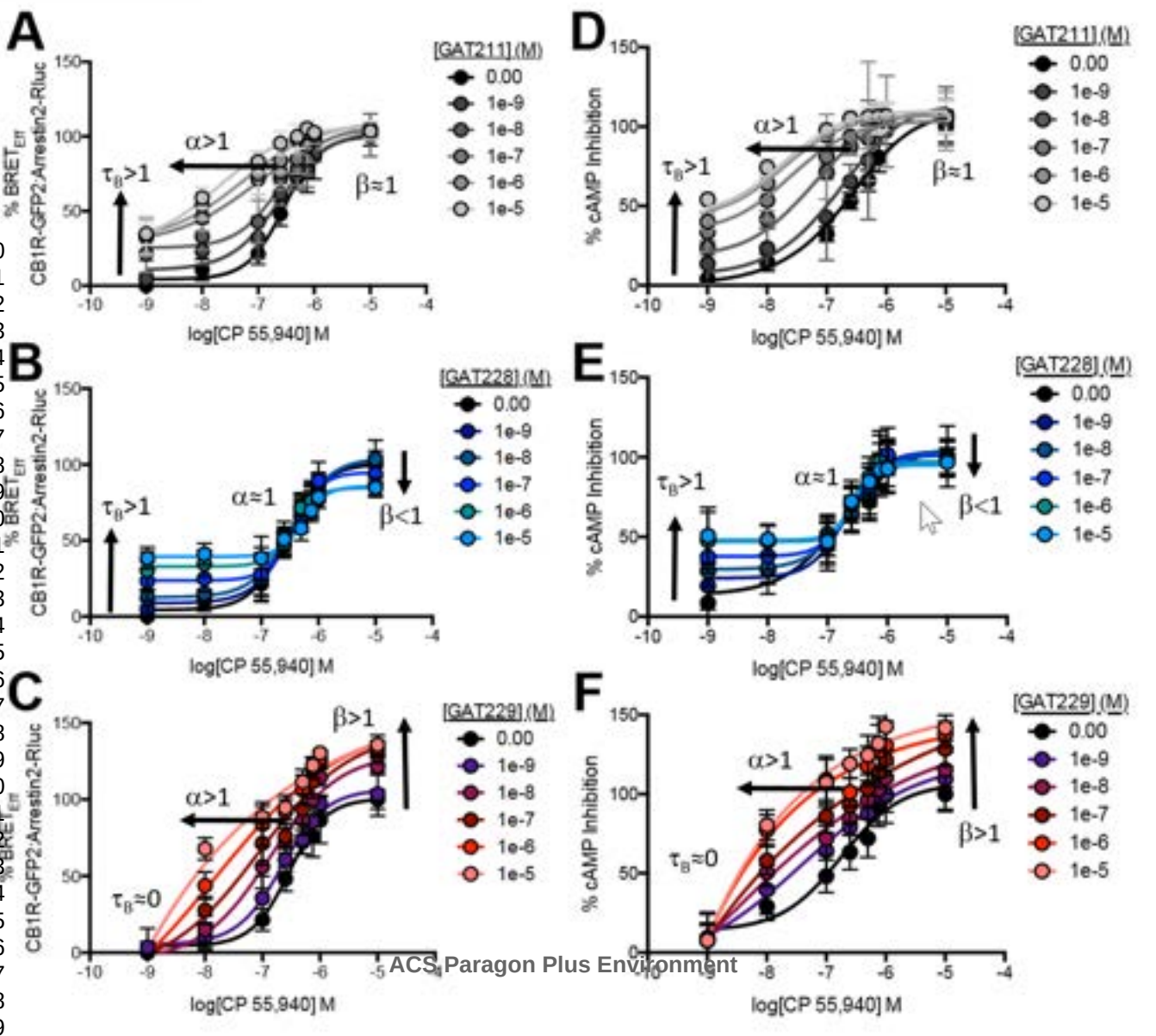
A
% BRET Eff
CB1R-GFP2:Arrestin2-Rluc
τB>1
α>1
β≈1
log[CP 55,940] M
[GAT211] (M)
0.00
1e-9
1e-8
1e-7
1e-6
1e-5
B
% BRET Eff
CB1R-GFP2:Arrestin2-Rluc
τB>1
α≈1
β<1
log[CP 55,940] M
[GAT228] (M)
0.00
1e-9
1e-8
1e-7
1e-6
1e-5
C
% BRET Eff
CB1R-GFP2:Arrestin2-Rluc
β>1
α>1
τB≈0
log[CP 55,940] M
[GAT229] (M)
0.00
1e-9
1e-8
1e-7
1e-6
1e-5
D
% cAMP Inhibition
τB>1
α>1
β≈1
log[CP 55,940] M
[GAT211] (M)
0.00
1e-9
1e-8
1e-7
1e-6
1e-5
E
% cAMP Inhibition
τB>1
α≈1
β<1
log[CP 55,940] M
[GAT228] (M)
0.00
1e-9
1e-8
1e-7
1e-6
1e-5
F
% cAMP Inhibition
α>1
β>1
τB≈0
log[CP 55,940] M
[GAT229] (M)
0.00
1e-9
1e-8
1e-7
1e-6
1e-5

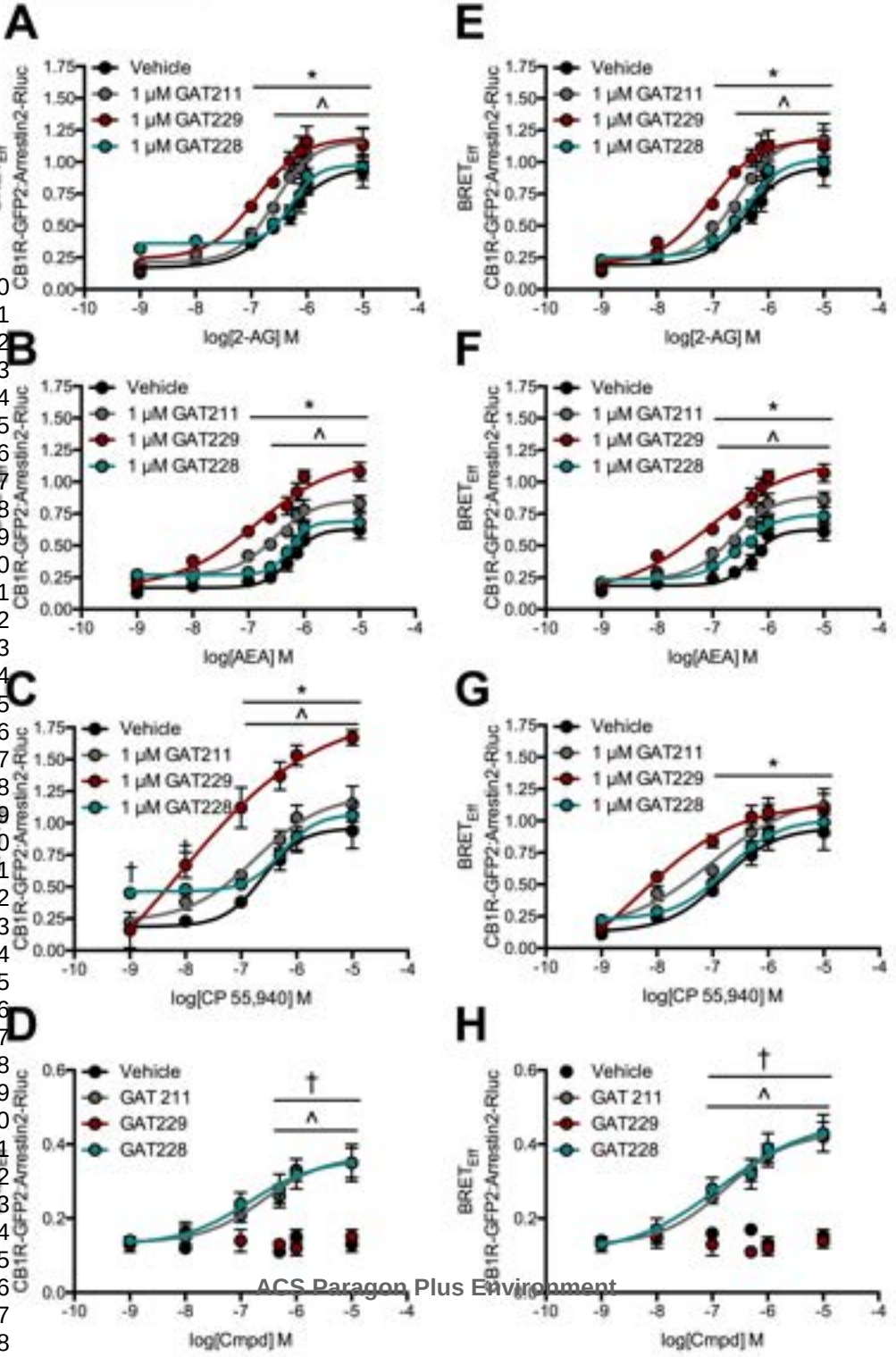
A
B
C
D
E
F
G
H
Vehicle
1 μM GAT211
1 μM GAT229
1 μM GAT228
GAT 211
GAT229
GAT228
BRET Eff
CB1R-GFP2:Arrestin2-Riluc
log[2-AG] M
log[AEA] M
log[CP 55,940] M
log[Cmpd] M
*
^
†
‡

Figure 8

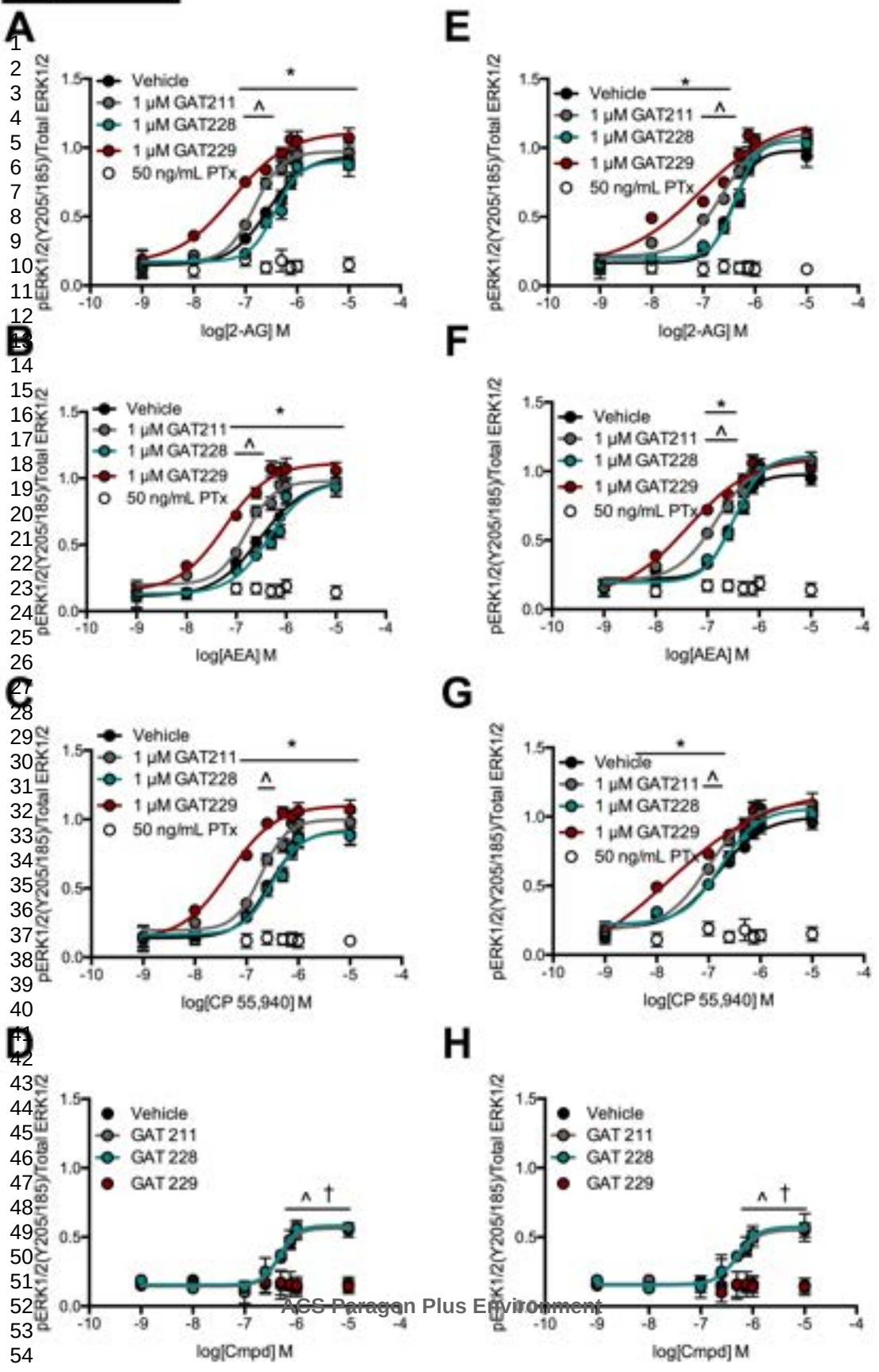
A
E
B
F
C
G
D
H
Vehicle
1 μM GAT211
1 μM GAT228
1 μM GAT229
50 ng/mL PTx
GAT 211
GAT 228
GAT 229
pERK1/2(Y205/185)/Total ERK1/2
log[2-AG] M
log[AEA] M
log[CP 55,940] M
log[Cmpd] M
*
^
†

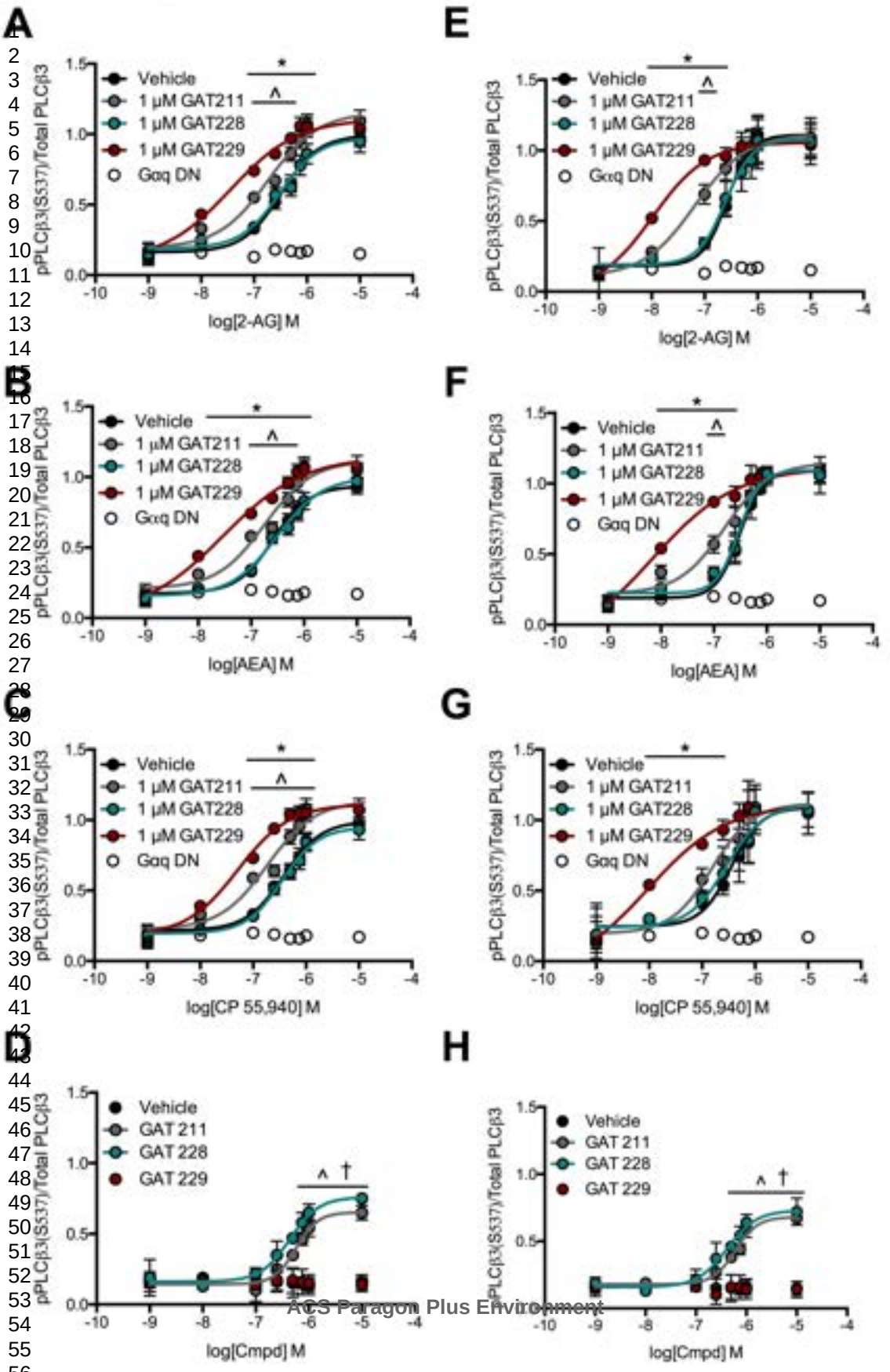

Figure 10

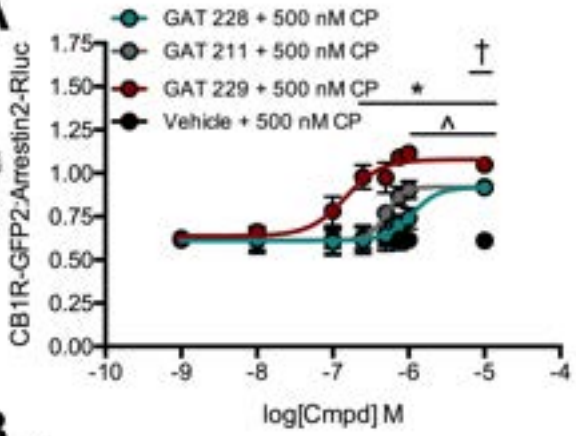

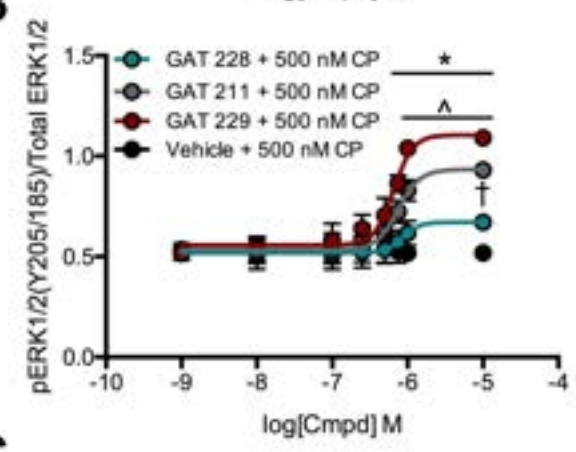

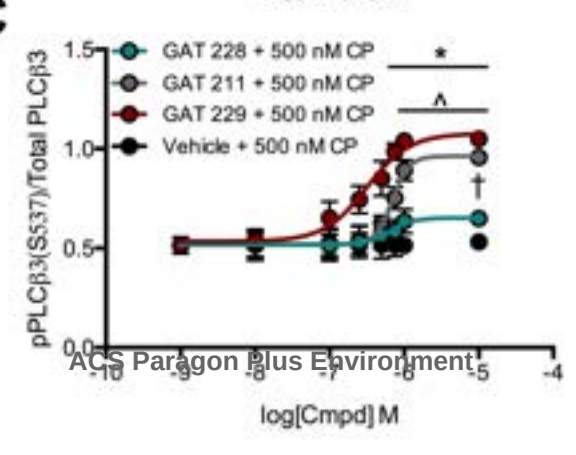

Figure 11

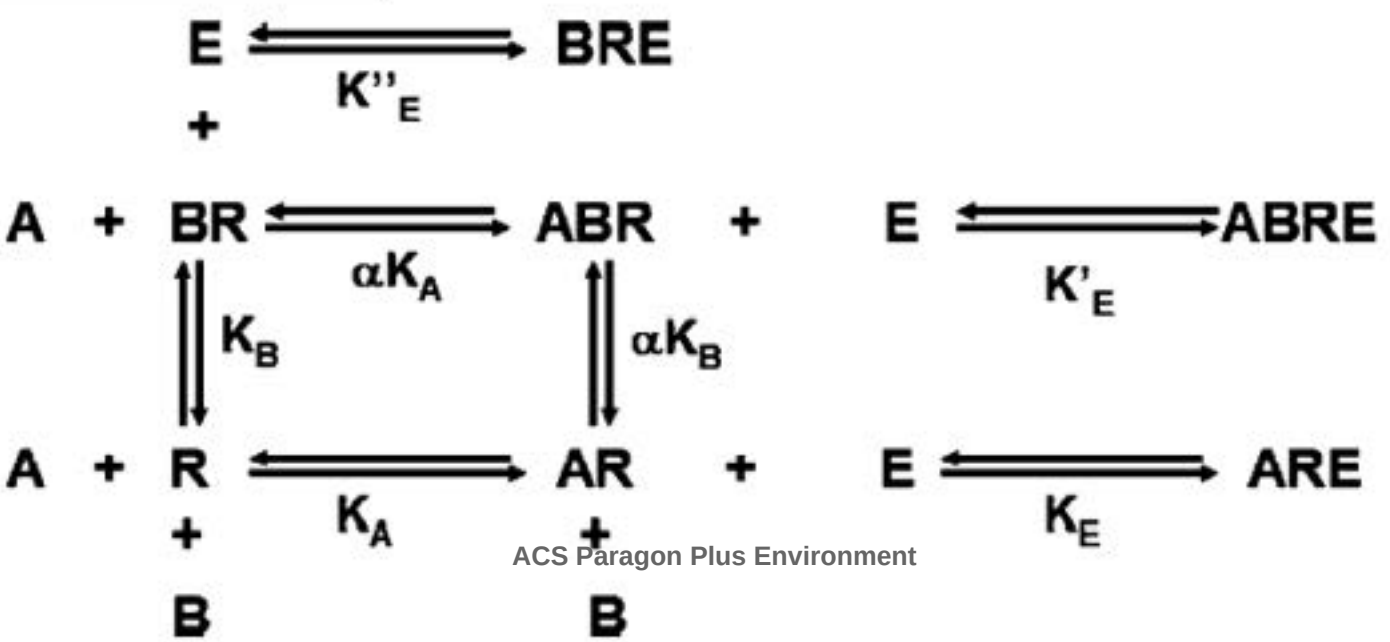

TABLES:

Table 1. Operational model of allosterism for GAT211, GAT228, and GAT229.

	$BRET_{Eff}$			cAMP		
	GAT211	**GAT228**	**GAT229**	**GAT211**	**GAT228**	**GAT229**
pK_B	7.26 ± 0.07	6.93 ± 0.09	6.99 ± 0.14	6.76 ± 0.08	7.4 ± 0.12	6.91 ± 0.27
α	24 ± 2.83	2.5 ± 0.58	4.25 ± 1.5	21 ± 2	1.08 ± 0.34	2.25 ± 1.26
β	0.95 ± 0.06	0.68 ± 0.09	2.3 ± 0.38	1.13 ± 0.19	0.95 ± 0.5	10.75 ± 4.43
Log(αβ)	1.35 ± 0.04	0.21 ± 0.10	0.97 ± 0.14	1.37 ± 0.06	-0.06 ± 0.36	1.3 ± 0.35
τ_B	0.15 ± 0.03	0.19 ± 0.04	0	0.19 ± 0.08	0.15 ± 0.06	0

All values estimated using the allosteric binding model[41, 42] combined with the Black –Leff operational model for agonism[43] for the data presented in Figure 6. Data are mean of 4 independent estimates of pK_B α, β, Log(αβ), and τ_B ± SD.

Table 2. Summary of induced bias for GAT211, GAT228, and GAT229.

	ΔLog(αβ)		Induced Bias	
GAT211	**0.01**	(-0.18 – 0.21)	**n.s**	
GAT228	**-0.27**	(-0.40 – -0.09)	**0.54**	(0.35 – 0.81)
GAT229	**0.34**	(0.14 – 0.54)	**2**	(1.4 – 3.47)

All values estimated using the allosteric binding model[41, 42] combined with the Black –Leff operational model for agonism[43] for the data presented in Figure 6. Data are mean of 4 independent experiments with 95% CI.

Table 3. Summary of data by assay for GAT211, GAT228, and GAT229.

	Arrestin2	
Compound	**EC_{50} (nM, 95% CI)**	**E_{max} (%) ± SEM**
GAT211	775 (656 – 896)	129.54 ± 13.23
GAT228	832 (652 – 101)	105.89 ± 4.85
GAT229	255 (97.0 – 417)†*	126.98 ± 12.19*
	ERK ($G\alpha_{i/o}$)	
	EC_{50} (nM. 95% CI)	**E_{max} (%) ± SEM**
GAT211	647 (516 – 776)	109.61 ± 16.11
GAT228	703 (558 – 855)	96.85 ± 5.14
GAT229	319 (133 – 520)†*	100.45 ± 3.60^
	PLCβ3 ($G\alpha_q$)	
	EC_{50} (nM, 95% CI)	**E_{max} (%) ± SEM**
GAT211	553 (354 – 737)	112.81 ± 14.21
GAT228	895 (765 – 1,029)	96.30 ± 6.29
GAT229	332 (160 – 503)*	118.55 ± 6.39*

EC_{50} determined using non-linear regression analysis; E_{max} maximum (%) effect compared to orthosteric agonist alone, determined using non-linear regression (4 parameter) analysis. Data are mean with 95% CI (EC_{50}) or ± SEM (E_{max}). Data were calculated as the mean of data for each assay in HEK293A cells in the presence of 500 nM CP55,940 (EC_{50}, Fig. 10) and HEK293A and Neuro2a cells treated with 2-AG, AEA or CP55,940 ± 1 μM GAT211, GAT228, or GAT229 (E_{max}, Figs. 7-9). †$P < 0.01$ compared to GAT211, *$P < 0.05$ compared to GAT228, within assay; ^$P < 0.05$ compared to arrestin2 within compound, as determined by non-overlapping CI or unpaired *t*-test.

Table 4. Summary of data by orthosteric probe for GAT211, GAT228, and GAT229.

	2-AG	
Compound	**EC_{50} (nM, 95% CI)**	**E_{max} (%) ± SEM**
GAT211	597 (526 – 686)	121.94 ± 7.90
GAT228	826 (708 – 966)	113.03 ± 9.22†
GAT229	268 (81.5 – 443)†*	136.16 ± 4.66†*
	AEA	
	EC_{50} (nM, 95% CI)	**E_{max} (%) ± SEM**
GAT211	606 (435 – 780)	124.79 ± 7.63
GAT228	715 (585 – 828)	113.81 ± 9.69†
GAT229	283 (158 – 413)†*	143.46 ± 4.37†*
	CP55,940	
	EC_{50} (nM, 95% CI)	**E_{max} (%) ± SEM**
GAT211	660 (526 – 804)	105.13 ± 1.74^
GAT228	750 (578 – 936)	90.28 ± 1.11†^
GAT229	360 (203 – 528)*	132.99 ± 4.11†*

EC_{50} determined using non-linear regression analysis; E_{max} maximum (%) effect compared to orthosteric agonist alone, determined using non-linear regression (4 parameter) analysis. Data are mean with 95% CI (EC_{50}) or ± SEM (E_{max}). Data were calculated as the mean of data for each assay in HEK293A cells in the presence of 500 nM CP55,940 (EC_{50}, Fig. 10) and HEK293A and Neuro2a cells treated with 2-AG, AEA or CP55,940 ± 1 μM GAT211, GAT228, or GAT229 (E_{max}, Figs. 7-9). †$P < 0.01$ compared to GAT211, *$P < 0.05$ compared to GAT228, within assay; ^$P < 0.05$ compared to arrestin2 within compound, as determined by non-overlapping CI or unpaired *t*-test.

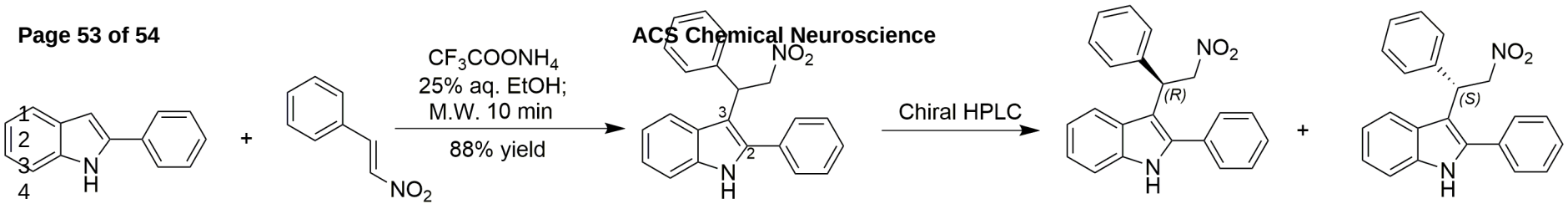

1
GA211
(racemic)

1a
GAT228
(+)-enantiomer
CB1 allosteric agonist

1b
GAT229
(-)-enantiomer
CB1 PAM

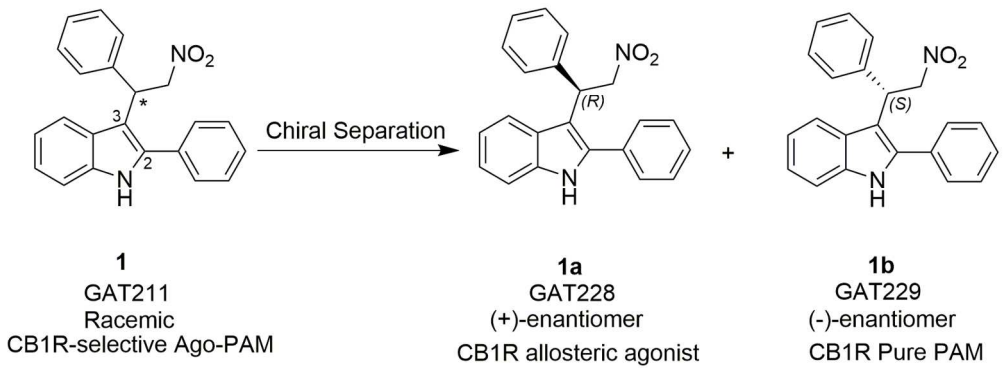

1
GAT211
Racemic
CB1R-selective Ago-PAM

1a
GAT228
(+)-enantiomer
CB1R allosteric agonist

1b
GAT229
(-)-enantiomer
CB1R Pure PAM

151x55mm (300 x 300 DPI)